

Electronic Supplementary Information (ESI) for

Nitrogen-Doped Heptazethrene and Octazethrene Diradicaloids

Chi Hao Eugene Chow,^a Yi Han,^a Hoa Phan,^a and Jishan Wu^{,a}*

^aDepartment of Chemistry, National University of Singapore, 3 Science Drive 3, 117543, Singapore

Table of Content

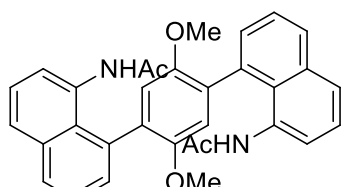
1. Experimental section	
1.1 General information.....	S2
1.2 Synthetic procedures and characterization data.....	S3
2. Additional spectral data.....	S9
3. Theoretical calculations.....	S14
4. X-ray crystallographic analysis.....	S18
5. Additional ¹ H/ ¹³ C NMR and mass spectra.....	S32
6. References.....	S47

1. Experimental Section

1.1. General information

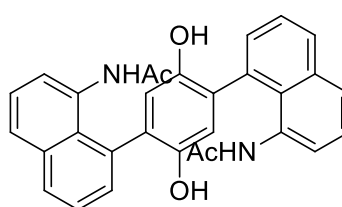
All reagents and starting materials were obtained from commercial suppliers and used without further purification. Anhydrous toluene and THF were distilled from sodium-benzophenone immediately prior to use. The ^1H NMR and ^{13}C NMR spectra were recorded in solution of CD_2Cl_2 , dimethyl sulfoxide- d_6 and benzene- d_6 on Bruker DPX 500 NMR spectrometers with tetramethylsilane (TMS) as the internal standard. The following abbreviations were used to explain the multiplicities: s = singlet, d = doublet, t = triplet, q = quartet, m = multiplet. HR-APCI mass spectra (MS) were recorded on Bruker amazon mass spectrometer. HR-ESI mass spectra were recorded on Finnigan LCQ quadrupole ion trap mass spectrometer. The solvents used for UV-vis are of HPLC grade (Merck). UV-vis absorption was recorded on a Shimadzu UV-3600 spectrophotometer. Cyclic voltammetry measurements were performed in dry dichloromethane on a CHI 620C electrochemical analyzer with a three-electrode cell, using 0.1 M tetrabutylammonium hexafluorophosphate (Bu_4NPF_6) as supporting electrolyte, AgCl/Ag as reference electrode, gold disk as working electrode, Pt wire as counter electrode and scan rate at 50 mV s^{-1} . The potential was externally calibrated against the ferrocene/ferrocenium couple. The single crystal was measured at low temperature ($T = 100 \text{ K}$) on a four circles goniometer Kappa geometry Bruker AXS D8 Venture equipped with a Photon 100 CMOS active pixel sensor detector using a Copper monochromatized ($\lambda = 1.54178 \text{ \AA}$) X-ray radiation. Continuous wave X-band ESR spectra were obtained with a JEOL (FA200) spectrometer. 1-acetamido-8-bromonaphthalene¹ and 2,5-dimethoxy-1,4-phenyldiboronic acid² were synthesized according to reported literatures.

1.2. Synthetic procedures and characterization data



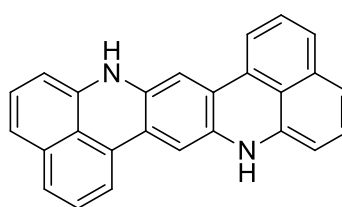
A mixture of 1-acetamido-8-bromonaphthalene (**1**, 660 mg, 2.5 mmol), 2,5-dimethoxy-1,4-phenyldiboronic acid (**2a**, 226 mg, 1.0 mmol), tetrakis(triphenylphosphine)palladium(0) (115 mg, 0.10 mmol) in dimethoxyethane (10 mL) and Na₂CO₃ aqueous solution (2 M, 5 mL) was degassed by three freeze-pump-thaw cycles. The reaction was heated at 115 °C for 48 h under nitrogen. After cooling to the room temperature, the precipitate was filtered off and washed with water and dried on the air to give compound

3a in 71% yield (358 mg). ¹H NMR (DMSO-*d*₆, 500 MHz): δ ppm 8.57 (s, 2H), 7.99 (d, 2H), 7.90 (d, 2H), 7.58 (t, 2H), 7.52 (t, 2H), 7.42 (d, 2H), 7.23 (d, 2H), 6.58 (s, 2H), 3.54 (s, 6H), 1.52 (s, 6H). ¹³C NMR (DMSO-*d*₆, 125 MHz): δ ppm 167.90 (C=O), 149.51, 134.73, 134.54, 134.02, 130.74, 129.30, 128.44, 127.80, 126.98, 125.38, 125.17, 125.09, 112.95, 55.57, 22.74. HR-MS analysis (APCI) [MH⁺]: 505.2113, theoretical mass for C₃₂H₂₉N₂O₄ [MH⁺]: 505.2122, err: 1.8 ppm.



Boron tribromide (0.4 mL, 4.0 mmol) was added to 10 mL dry CH₂Cl₂ solution of **3a** (505 mg, 1.0 mmol) under nitrogen at 0 °C. The mixture was stirred for 48 h at room temperature and then poured into water. The precipitate was filtered off and washed with large amount of water and dried on air to give compound **4a**

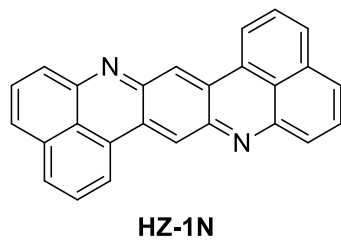
in 72% yield (373 mg). ¹H NMR (DMSO-*d*₆, 500 MHz): δ ppm 8.85 (s, 2H), 8.56 (s, 2H), 7.97 (d, 2H), 7.86 (d, 2H), 7.58 (m, 4H), 7.51 (t, 2H), 7.19 (d, 2H), 6.74 (s, 2H), 1.61 (s, 6H). ¹³C NMR (DMSO-*d*₆, 125 MHz): δ ppm 167.78 (C=O), 146.76, 134.73, 134.64, 134.11, 129.66, 129.35, 128.38, 126.80, 126.46, 125.33, 125.15, 123.42, 116.68, 22.95. HR-MS analysis (APCI) [MH⁺]: 477.1808, theoretical mass for C₃₀H₂₅N₂O₄ [MH⁺]: 477.1809, err: 0.2 ppm.



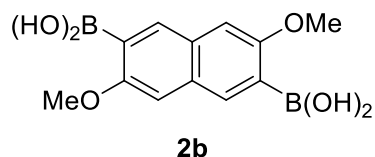
A solution of **4a** (238 mg, 0.5 mmol) in a mixture of dimethyl sulfoxide (DMSO) (10 mL), propan-2-ol (5 mL) and hydrazine hydrate (80%, 10 mL) was stirred under nitrogen at 140 °C for 72 h. The mixture was poured into water (100 mL) and extracted with CH₂Cl₂. The organic layer was dried over Na₂SO₄. The solvent was removed under vacuum and residue was purified by silica gel column chromatography using CH₂Cl₂/hexane (1/2, v/v) as eluent to give compound **5a** as a red powder

in 22% yield (39 mg). ¹H NMR (CD₂Cl₂, 500 MHz): δ ppm 7.82 (s, 2H), 7.46 (m, 2H), 7.30

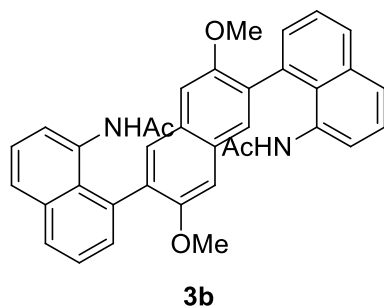
(m, 6H), 7.01 (s, 2H), 6.67 (t, 2H), 3.98 (s, 2H). Due to its poor solubility, ^{13}C NMR spectrum was not recorded. HR-MS analysis (APCI) [MH $^+$]: 357.1382, theoretical mass for C₂₆H₁₇N₂ [MH $^+$]: 357.1386, err: 1.2 ppm.



Lead(IV) oxide (50 mg, 0.2 mmol) was added into 0.5 mL dry CH₂Cl₂ solution of **5a** (3.5 mg, 10 μmol) under nitrogen. The reaction mixture was allowed to stir for 30 mins. The color of the reaction mixture changed from red to deep blue. Insoluble inorganic residue was filtered off and the solvent was removed under vacuum to give **HZ-1N**, which immediately decomposed upon contact with moisture. The in situ generated solution was used for UV-vis measurement.



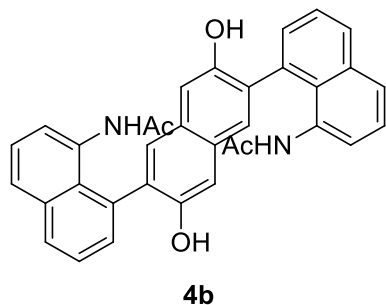
To a solution of 2,6-dimethoxynaphthalene (1.88 g, 10 mmol) in dry THF (60 mL), *n*-butyllithium solution (20 mL, 40 mmol, 2.0 M in cyclohexane) was added dropwise in 30 minutes at room temperature under nitrogen. The mixture was allowed to stir for 5 h and trimethyl borate (11.2 mL, 100 mmol) was added slowly at -78 °C. The resulted solution was stirred overnight and allowed to warm slowly to room temperature. The mixture was decomposed with 10% HCl (50 mL) and extracted with CH₂Cl₂. The extract was dried over Na₂SO₄. The solvent was removed under vacuum and the crude product was recrystallized from H₂O/CH₃CN (1/1, v/v) mixture, affording white needles of the product **2b** (1.1 g) in 39% yield. ^1H NMR (DMSO-*d*₆, 500 MHz): δ ppm 7.99 (s, 2H), 7.87 (s, 4H), 7.24 (s, 2H), 3.87 (s, 6H). ^{13}C NMR (DMSO-*d*₆, 125 MHz): δ ppm 159.03, 134.49, 130.05, 104.87, 55.21. HR-MS analysis (ESI) [MH $^+$]: 299.0874, theoretical mass for C₁₂H₁₄B₂NaO₆ [MH $^+$]: 299.0873, err: -0.4 ppm.



A mixture of 1-acetamido-8-bromonaphthalene (660 mg, 2.5 mmol), compound **2b** (276 mg, 1.0 mmol), tetrakis(triphenylphosphine)palladium(0) (115 mg, 0.10 mmol) in dimethoxyethane (10 mL) and Na₂CO₃ aqueous solution (2 M, 5 mL) was degassed by three freeze-pump-thaw cycles. The reaction was heated at 115 °C for 48 h under nitrogen.

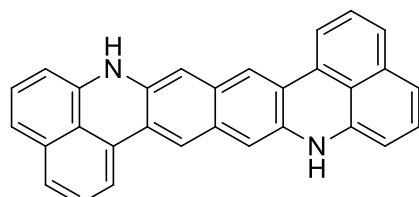
After cooling to the room temperature, the precipitate was filtered off and washed with water and dried on the air to give compound **3b** in 65% yield (360 mg) which has two atropisomers. ^1H NMR (DMSO-*d*₆, 500 MHz): δ ppm 8.61 (s, 2H), 7.99 (d, 2H), 7.91 (d, 2H), 7.70 (s, 2H), 7.53 (m, 4H), 7.29 (m, 6H), 3.63 (s, 6H), 1.08 (s, 6H). ^{13}C NMR (DMSO-*d*₆, 125 MHz): δ ppm

168.09 (C=O), 167.94 (C=O), 154.22, 154.18, 134.84, 134.81, 134.56, 134.46, 134.39, 134.29, 134.16, 133.85, 130.65, 130.03, 128.60, 128.55, 128.49, 128.48, 128.39, 127.10, 127.07, 127.01, 126.84, 125.36, 125.23, 125.17, 125.14, 124.59, 104.38, 104.26, 55.16, 55.09, 22.77, 22.11. HR-MS analysis (APCI) [MH⁺]: 555.2276, theoretical mass for C₃₆H₃₁N₂O₄ [MH⁺]: 555.2278, err: 0.4 ppm.



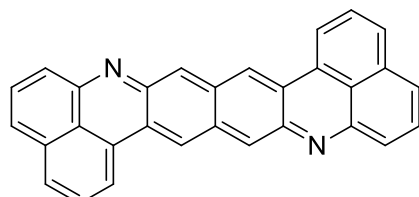
Boron tribromide (0.4 mL, 4.0 mmol) was added to 10 mL dry CH₂Cl₂ solution of **3b** (555 mg, 1.0 mmol) under nitrogen at 0 °C. The mixture was stirred for 48 h at room temperature and then poured into water. The precipitate was filtered off and washed with large amount of water and dried on air to give compound **4b** in 69% yield (364 mg) which has two atropisomers.

¹H NMR (DMSO-*d*₆, 500 MHz): δ ppm 8.61 (s, 2H), 7.99 (d, 2H), 7.91 (d, 2H), 7.70 (s, 2H), 7.54 (m, 4H), 7.30 (m, 6H), 1.08 (s, 6H). Due to its poor solubility, ¹³C NMR spectrum was not recorded. HR-MS analysis (APCI) [MH⁺]: 527.1964, theoretical mass for C₃₄H₂₇N₂O₄ [MH⁺]: 527.1965, err: 0.3 ppm.



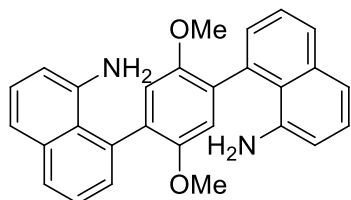
A solution of **4b** (238 mg, 0.5 mmol) in a mixture of dimethyl sulfoxide (DMSO) (10 mL), propan-2-ol (5 mL) and hydrazine hydrate (80%, 10 mL) was stirred under nitrogen at 140 °C for 72 h. The mixture was poured into water (100 mL) and extracted with CH₂Cl₂. The organic

layer was dried over Na₂SO₄. The solvent was removed under vacuum and residue was purified by silica gel column chromatography using CH₂Cl₂/hexane (1/2, v/v) as eluent to give compound **5b** as a red powder in 15% yield (30 mg). ¹H NMR (CD₂Cl₂, 500 MHz): δ ppm 7.97 (d, 2H), 7.83 (d, 2H), 7.81 (s, 2H), 7.56 (t, 2H), 7.53 (t, 2H), 7.37 (d, 2H), 7.30 (s, 2H), 7.13 (m, 2H), 3.78 (s, 2H). Due to its poor solubility, ¹³C NMR spectrum was not recorded. HR-MS analysis (ESI) [MH⁺]: 406.1473, theoretical mass for C₃₀H₁₈N₂ [MH⁺]: 406.1465, err: -2.2 ppm.



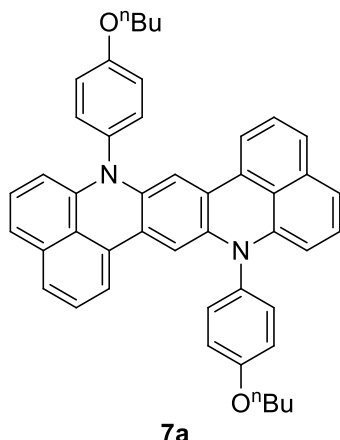
Lead(IV) oxide was added into 0.5 mL dry CH₂Cl₂ solution of **5b** (4.0 mg, 10 µmol) under nitrogen. The reaction mixture was allowed to stir for 30 mins. The color of the reaction mixture changed from red to colorless. Insoluble inorganic residue was filtered off and the solvent was

removed under vacuum to give **OZ-1N**, which immediately decomposed upon contact with moisture. The in situ generated solution was used for UV-vis measurement.



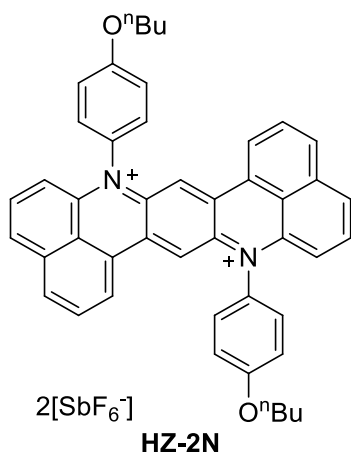
6a

A solution of **3a** (505 mg, 1.0 mmol) in a mixture of ethanol (7.0 mL) and concentrated HCl (37%, 3.0 mL) was stirred under reflux for 38 h. After cooling to the room temperature, the precipitate was filtered off and washed with large amount of water and dried on the air to give compound **6a** in 89% yield (378 mg) which has two atropisomers. ¹H NMR (CD_2Cl_2 , 500 MHz): δ ppm 7.85 (m, 2H), 7.48 (t, 2H), 7.40 (m, 2H), 7.33 (m, 2H), 7.21 (m, 2H), 7.05 (s, 2H), 6.88 (m, 2H), 3.62 (s, 6H). Due to its poor solubility, ¹³C NMR spectrum was not recorded. HR-MS analysis (APCI) [MH⁺]: 421.1912, theoretical mass for $\text{C}_{28}\text{H}_{25}\text{N}_2\text{O}_2$ [MH⁺]: 421.1911, err: -0.4 ppm.

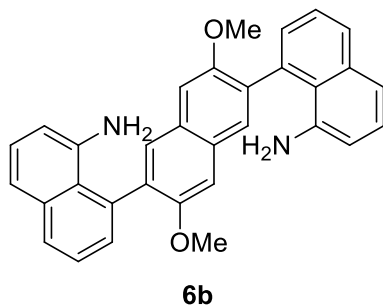


7a

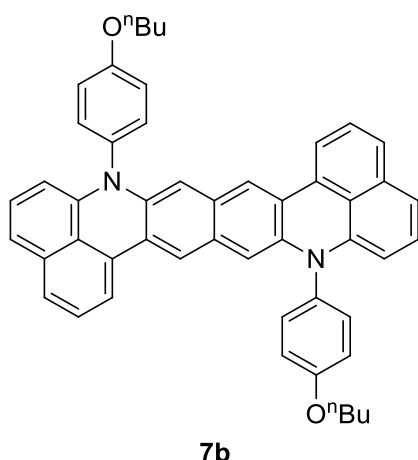
A mixture of **6a** (421 mg, 1.0 mmol), 1-bromo-4-butoxybenzene (504 mg, 2.2 mmol), bis(*tri-tert*-butylphosphine)palladium(0) (51 mg, 0.10 mmol) and sodium *tert*-butoxide (769 mg, 8.0 mmol) in toluene (20 mL) was degassed by three freeze-pump-thaw cycles. The reaction was heated at 130 °C for 24 h under nitrogen. After cooling to room temperature, the mixture was washed with water and extracted with CH_2Cl_2 . The organic layer was dried over anhydrous Na_2SO_4 . The solvent was removed under vacuum and the residue was purified by silica gel column chromatography using $\text{CH}_2\text{Cl}_2/\text{hexane}$ (1/4, v/v) as eluent to give compound **7a** as a red powder in 18% yield (117 mg). ¹H NMR ($\text{CS}_2/\text{C}_6\text{D}_6$, 20/1, v/v, 500 MHz): δ ppm 7.15 (d, 2H), 7.12 (d, 4H), 7.07 (d, 4H), 7.01 (t, 2H), 6.78 (m, 6 H), 6.54 (s, 2H), 5.64 (d, 2H), 3.99 (t, 4H), 1.80 (m, 4H), 1.53 (m, 4H), 1.00 (t, 6H). ¹³C NMR ($\text{CS}_2/\text{C}_6\text{D}_6$, 20/1, v/v, 125 MHz): δ ppm 159.32, 142.02, 137.32, 136.08, 132.83, 131.95, 129.80, 127.55, 127.31, 125.33, 123.95, 122.84, 117.39, 116.93, 113.95, 109.13, 105.43, 68.11, 32.08, 20.18, 14.59. HR-MS analysis (APCI) [MH⁺]: 653.3178, theoretical mass for $\text{C}_{46}\text{H}_{41}\text{N}_2\text{O}_2$ [MH⁺]: 653.3163, err: -2.3 ppm.



NOSbF₆ (2.9 mg, 11 μmol) dissolved in dry acetonitrile (10 μL) was added into 0.5 mL dry CH₂Cl₂ solution of **7a** (3.3 mg, 5 μmol) under nitrogen. The reaction mixture was allowed to stir for 5 mins. The color of the reaction mixture changed from red to deep blue. The solvent was removed under vacuum to give the dication **HZ-2N** without further purification. Due to its instability under ambient condition, its mass spectrum was not characterized. ¹H NMR (CD₂Cl₂, 500 MHz): δ ppm 8.49 (d, 4H), 8.31 (d, 2H), 8.25 (s, 2H), 8.07 (t, 2H), 7.78 (t, 2H), 7.66 (d, 4H), 7.50 (d, 2H), 7.39 (d, 4H), 4.20 (t, 4H), 1.92 (m, 4H), 1.60 (m, 4H), 1.05 (t, 6H).

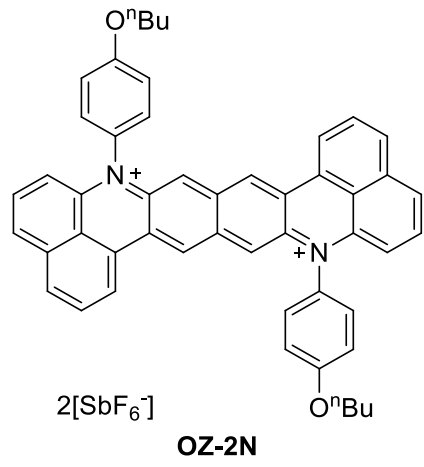


A solution of **3b** (555 mg, 1.0 mmol) in a mixture of ethanol (7.0 mL) and concentrated HCl (37%, 3.0 mL) was stirred under reflux for 38 h. After cooling to the room temperature, the precipitate was filtered off and washed with large amount of water and dried on the air to give compound **6b** in 88% yield (414 mg) which has two atropisomers. ¹H NMR (DMSO-*d*₆, 500 MHz): δ ppm 7.88 (d, 2H), 7.86 (s, 2H), 7.50 (s, 2H), 7.47 (m, 4H), 7.34 (t, 2H), 7.22 (d, 2H), 6.90 (m, 2H), 3.73 (s, 6H). ¹³C NMR (DMSO-*d*₆, 125 MHz): δ ppm 154.03, 153.98, 135.19, 135.16, 133.99, 133.73, 128.64, 128.60, 128.47, 128.29, 126.20, 124.91, 124.87, 106.26, 106.22, 55.58. HR-MS analysis (APCI) [MH⁺]: 471.2057, theoretical mass for C₃₂H₂₇N₂O₂ [MH⁺]: 471.2067, err: 2.2 ppm.



A mixture of **6b** (471 mg, 1.0 mmol), 1-bromo-4-butoxybenzene (504 mg, 2.2 mmol), bis(*tri-tert*-butylphosphine)palladium(0) (51 mg, 0.10 mmol) and sodium *tert*-butoxide (769 mg, 8.0 mmol) in toluene (20 mL) was degassed by three freeze-pump-thaw cycles. The reaction was heated at 130 °C for 24 h under nitrogen. After cooling to room temperature, the mixture was washed with water and extracted with CH₂Cl₂. The organic layer was dried over anhydrous Na₂SO₄. The solvent was removed under vacuum and the residue was purified by silica gel column chromatography using CH₂Cl₂/hexane (1/4, v/v) as eluent to give compound **7b** as a red powder in 7% yield (52 mg). ¹H NMR (CS₂/C₆D₆, 20/1, v/v, 500 MHz): δ ppm 7.81 (s, 2H), 7.64 (d, 2H), 7.43 (d, 2H), 7.32

(t, 2H), 7.24 (d, 4H), 7.18 (d, 4H), 6.97 (m, 4H), 6.38 (s, 2H), 5.86 (t, 2H), 3.99 (t, 4H), 1.81 (m, 4H), 1.54 (m, 4H), 1.01 (t, 6H). Due to its poor solubility, ^{13}C NMR spectrum was not recorded. HR-MS analysis (APCI) [MH $^+$]: 703.3330, theoretical mass for C₅₀H₄₃N₂O₂ [MH $^+$]: 703.3319, err: -1.6 ppm.



NO₂SbF₆ (3.1 mg, 11 μmol) dissolved in dry acetonitrile (10 μL) was added into 0.5 mL dry CH₂Cl₂ solution of **7b** (3.5 mg, 5 μmol) under nitrogen. The reaction mixture was allowed to stir for 5 mins. The color of the reaction mixture changed from red to dark green. The *in situ* generated solution was subject to UV-vis absorption measurement, which is in accordance with a structure of **OZ-2N**. After removing the solvent under vacuum, the hydrogenated dication **OZ-2N-H** was obtained. ^1H NMR (CD₂Cl₂, 500 MHz): δ ppm 9.29 (s, 2H), 8.85 (d, 2H), 8.29 (t, 2H), 8.10 (s, 2H), 8.03 (d, 2H), 7.68 (m, 2H), 7.52 (d, 4H), 7.42 (d, 4H), 6.87 (d, 2H), 4.53 (m, 4H), 4.25 (t, 4H), 1.94 (m, 4H), 1.64 (m, 4H), 1.10 (t, 6H).

2. Additional spectral data

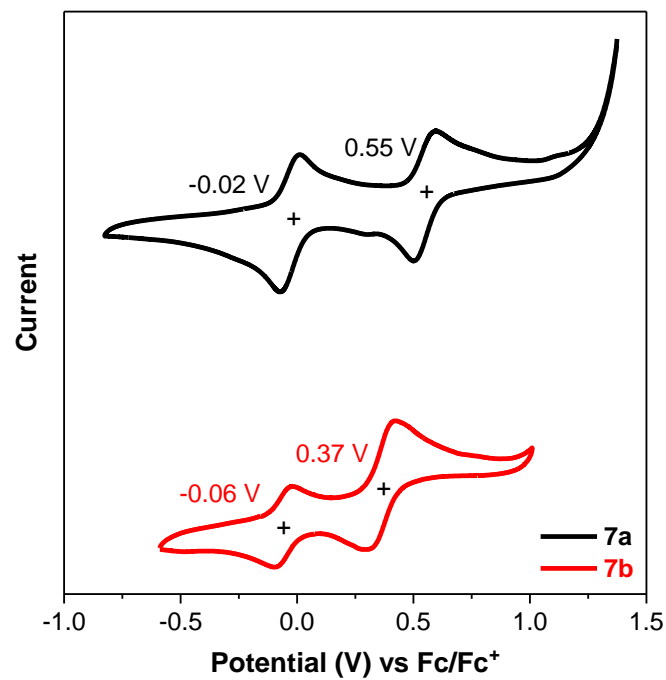


Fig. S1 Cyclic voltammograms of **7a** and **7b** (in CH_2Cl_2 ; $c = 1 \text{ mM}$) with $0.1 \text{ M Bu}_4\text{NPF}_6$ as supporting electrolyte, Ag/AgCl as the reference electrode, Pt wire as the counter electrode, and a scan rate at 50 mV s^{-1} .

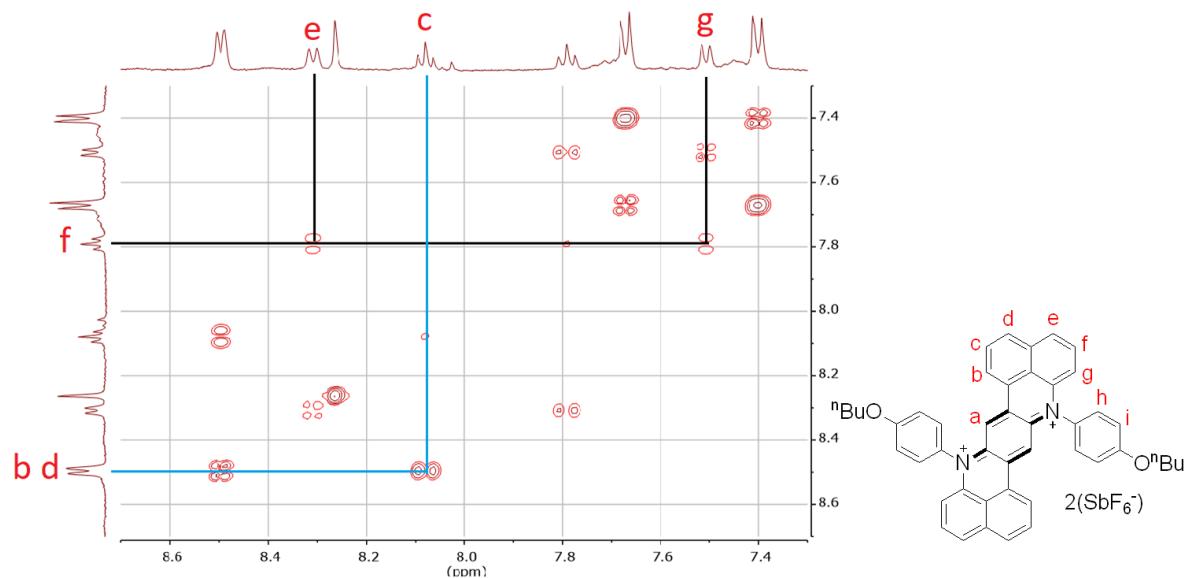


Fig. S2 2D COSY spectrum of **HZ-2N** (500 MHz, CD_2Cl_2 , -10°C).

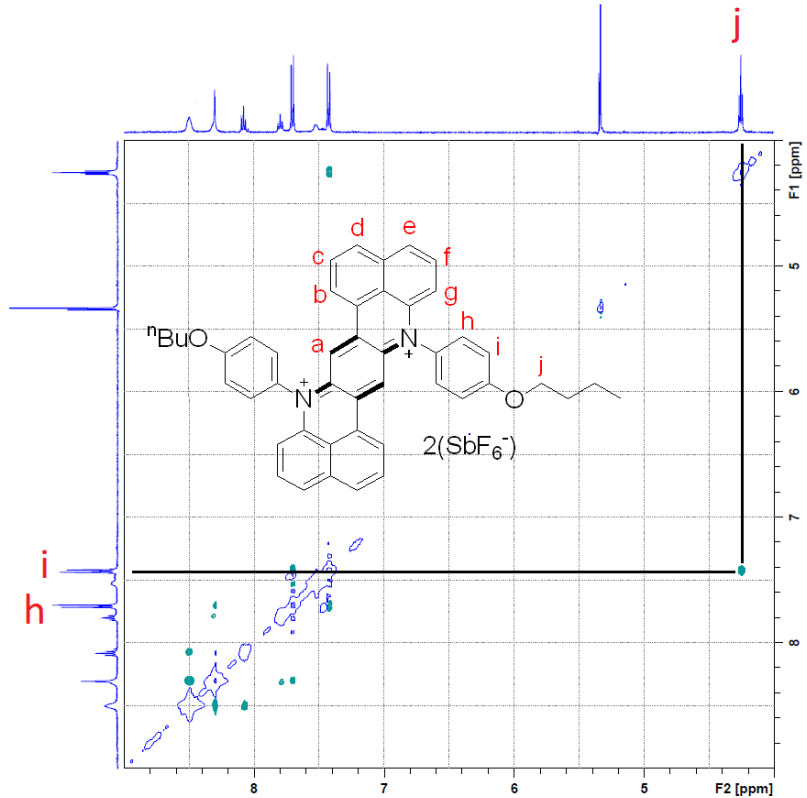


Fig. S3 2D NOESY spectrum of **HZ-2N** (500 MHz, CD_2Cl_2 , rt).

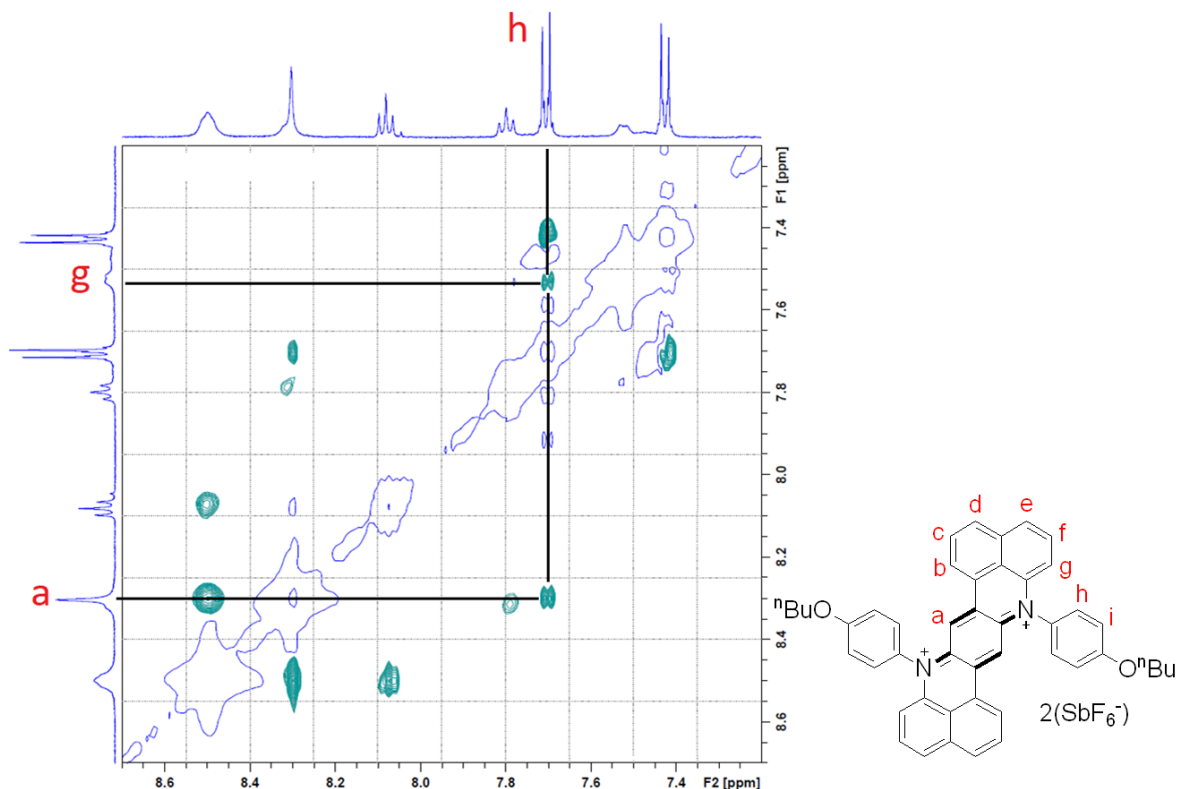


Fig. S4 2D NOESY spectrum of **HZ-2N** in aromatic region (500 MHz, CD_2Cl_2 , rt).

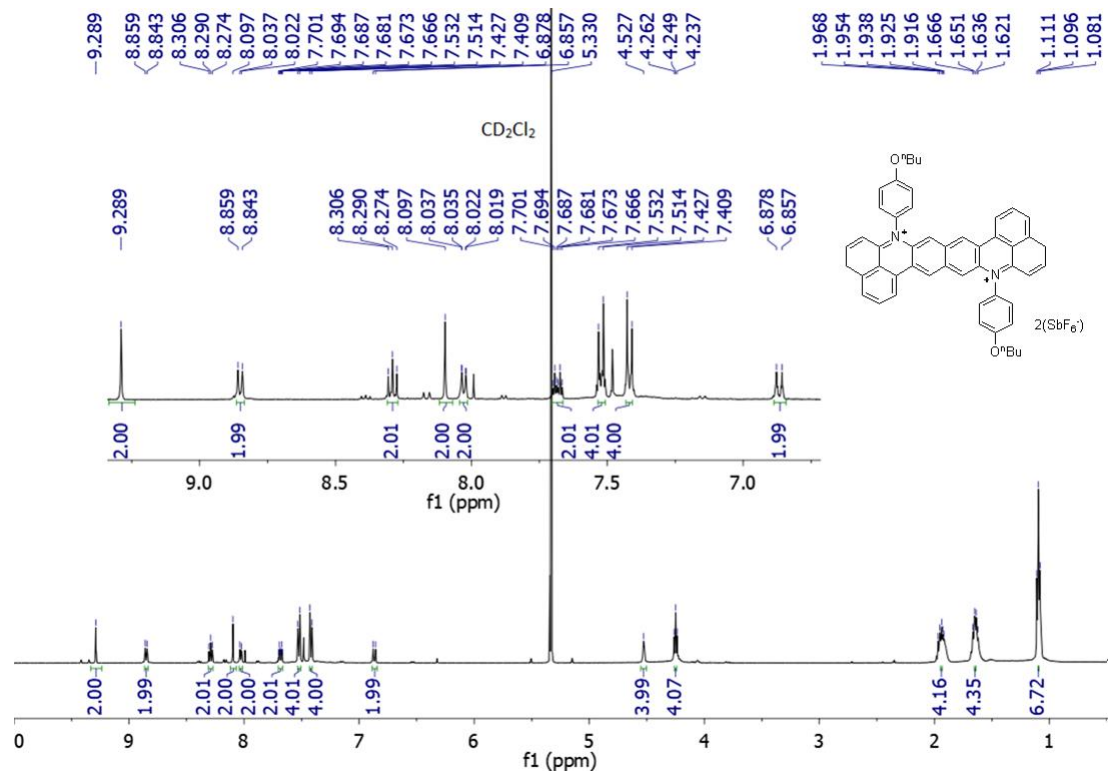


Fig. S5 ¹H NMR spectrum of **OZ-2N-H** (500 MHz, CD₂Cl₂, rt).

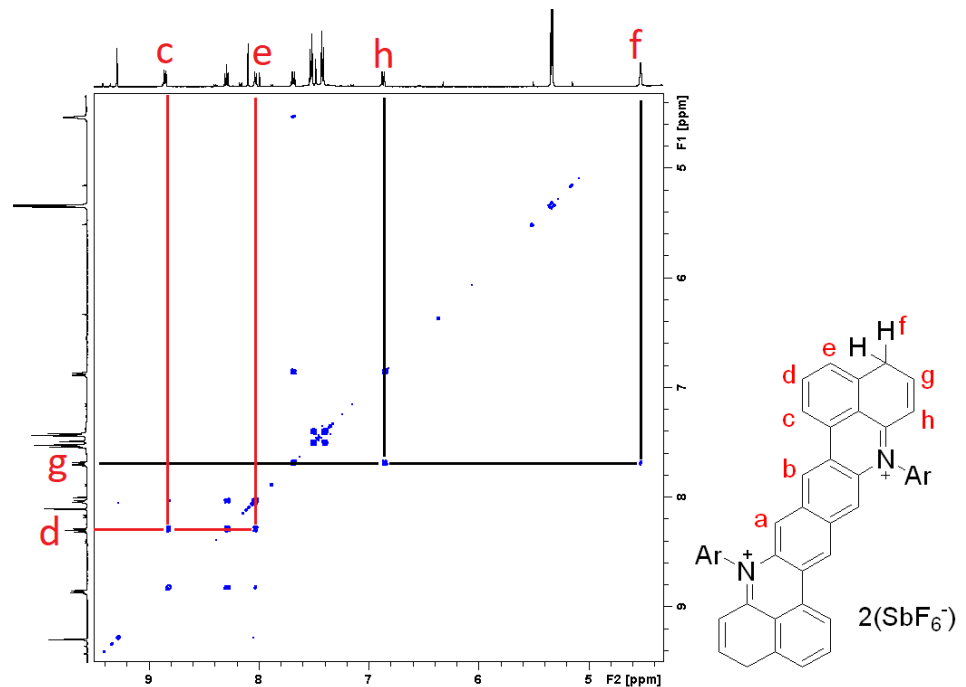


Fig. S6 2D COSY spectrum of **OZ-2N-H** (500 MHz, CD₂Cl₂, rt), Ar = 4-butoxyphenyl.

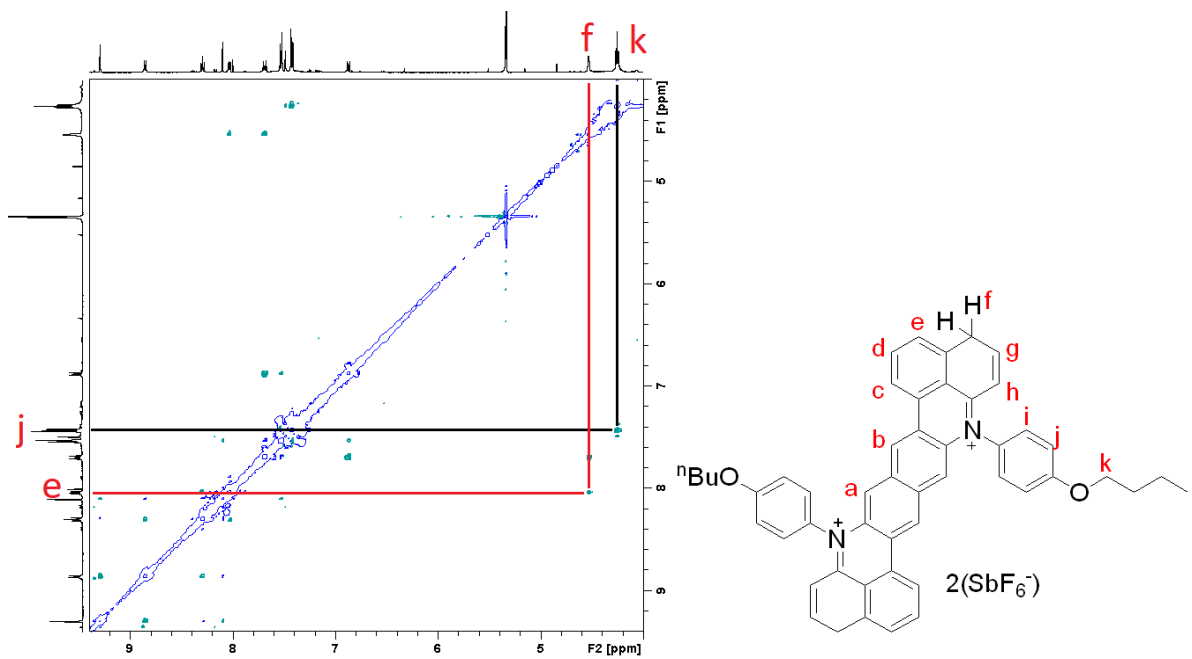


Fig. S7 2D NOESY spectrum of **OZ-2N-H** (500 MHz, CD₂Cl₂, rt).

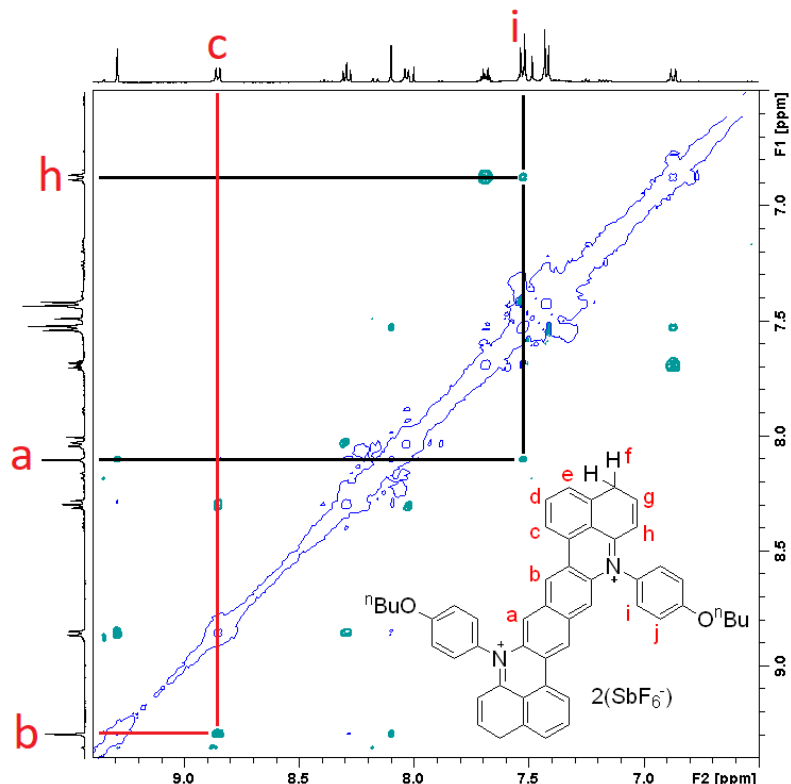


Fig. S8 2D NOESY spectrum of **OZ-2N-H** in aromatic region (500 MHz, CD₂Cl₂, rt).

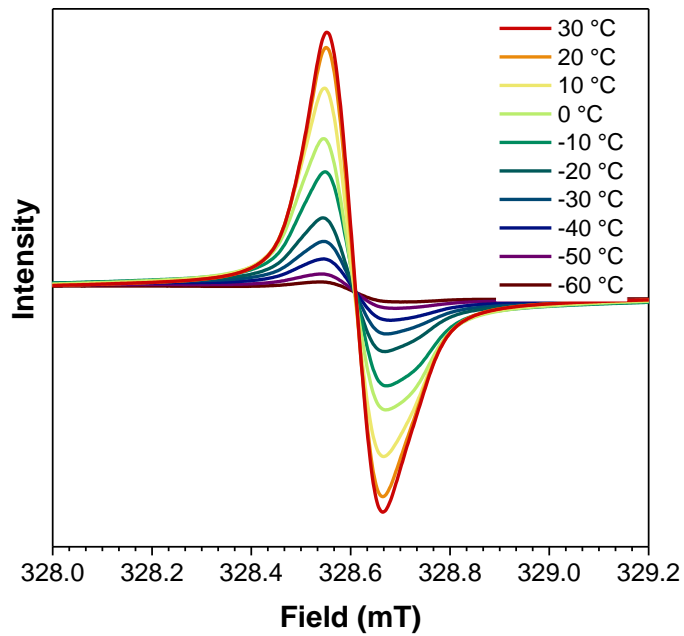


Fig. S9 Variable-temperature ESR spectra of **HZ-2N** in powder.

3. Theoretical calculations

Theoretical calculations were performed with the Gaussian09 rev. D program suite.³ All calculations were carried out using the density functional theory (DFT) method with Becke's three-parameter hybrid exchange functionals and the Lee-Yang-Parr correlation functional (B3LYP) employing the 6-31G(d,p) basis set for all atoms.⁴ NOON (natural orbital occupation number) calculations were done by spin unrestricted UCAM-B3LYP/6-31G(d,p) method and the diradical character (y_0) was calculated according to Yamaguchi's scheme: $y_0 = 1 - (2T/(1 + T^2))$, and $T = (n_{\text{HOMO}} - n_{\text{LUMO}})/2$ (n_{HOMO} is the occupation number n of the HOMO, n_{LUMO} is the occupation number n of the LUMO).⁵ Time-dependent (TD) DFT calculations were done based on RB3LYP/6-31G(d,p) with CPCM as solvation method.

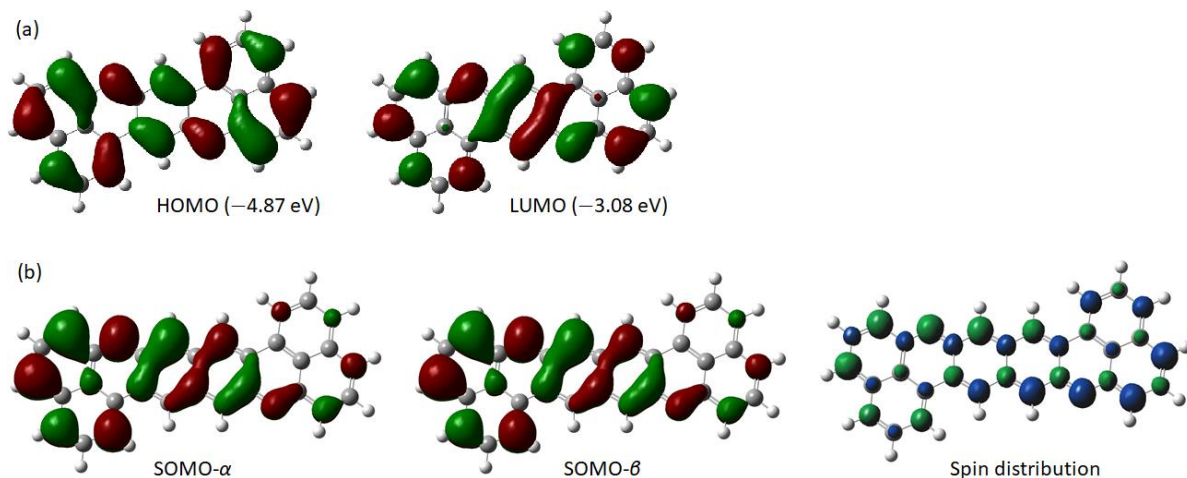


Fig. S10 (a) Calculated (RB3LYP/6-31G(d,p)) HOMO and LUMO for **HZ-1N** and (b) calculated (UCAM-B3LYP/6-31G(d,p)) SOMO- α and SOMO- β profiles and spin density distribution maps (α spin – β spin) for **OZ-1N**.

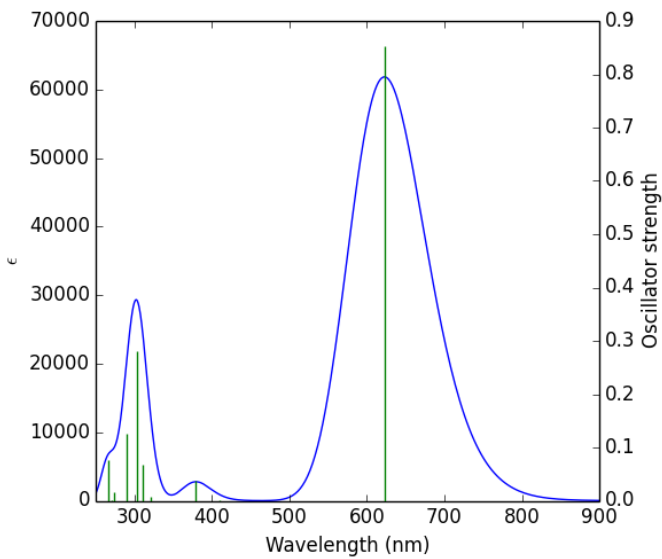


Fig. S11 TD DFT simulated spectrum of **HZ-1N**.

Table S1 Selected TD-DFT (RB3LYP/8-31G) calculated energies, oscillator strength and compositions of major electronic transitions of **HZ-1N**.

Wavelength (nm)	Oscillator strength	Major contribution
304.1	0.2812	H-1 → L+1 (93%)
379.5	0.038	H-3 → LUMO (90%)
622.8	0.8534	HOMO → LUMO (100%)

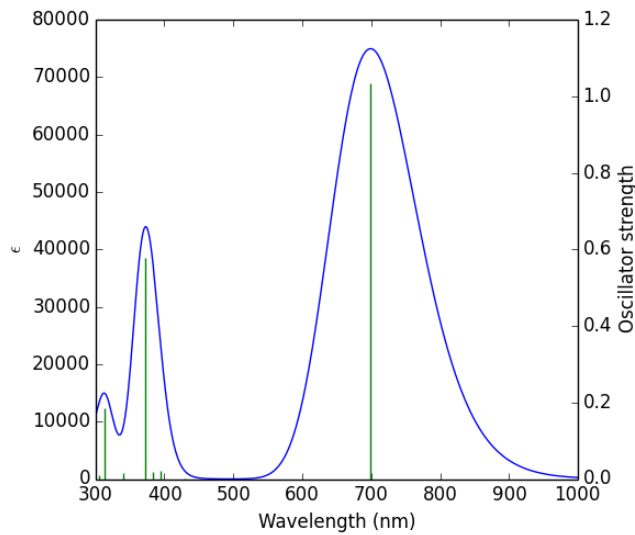


Fig. S12 TD DFT simulated spectrum of **OZ-1N**.

Table S2 Selected TD-DFT (RB3LYP/8-31G) calculated energies, oscillator strength and compositions of major electronic transitions of **OZ-1N**.

Wavelength (nm)	Oscillator strength	Major contribution
314.0	0.1839	HOMO → L+4 (77%)
372.3	0.5573	H-1 → L+1 (88%)
699.0	1.0342	HOMO → LUMO (100%)

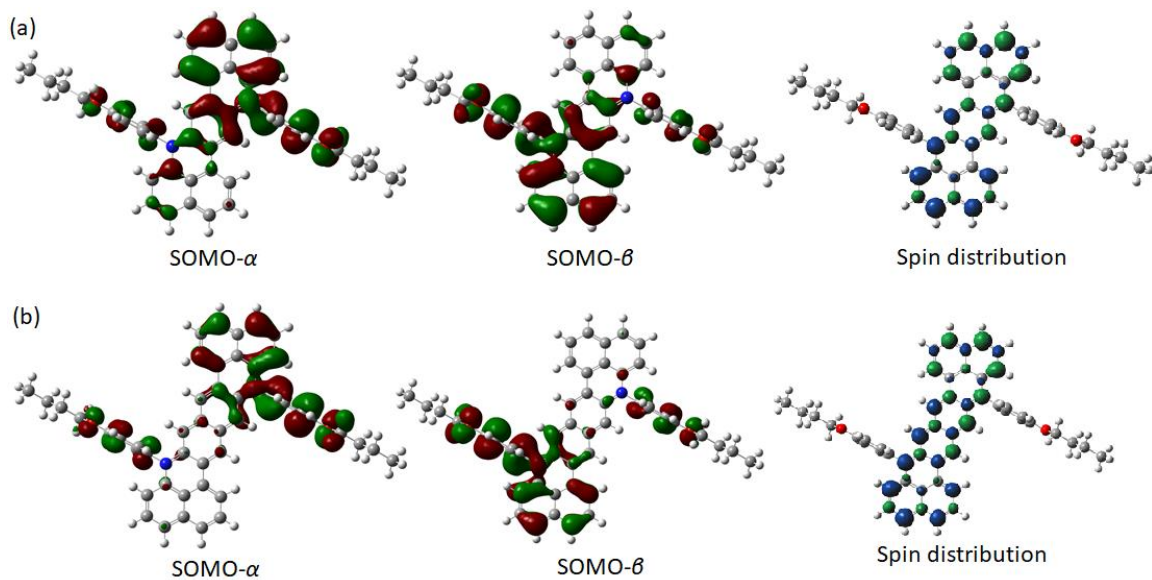


Fig. S13 Calculated (UCAM-B3LYP/6-31G(d,p)) SOMO- α and SOMO- β profiles and spin density distribution maps (α spin – β spin) for (a) **HZ-2N** and (b) **OZ-2N**.

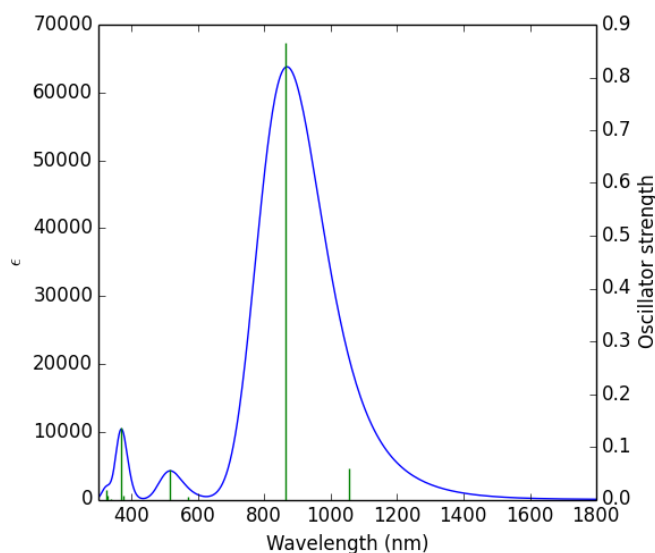


Fig. S14 TD DFT simulated spectrum of **HZ-2N**.

Table S3 Selected TD-DFT (rB3LYP/8-31G) calculated energies, oscillator strength and compositions of major electronic transitions of **HZ-2N**.

Wavelength (nm)	Oscillator strength	Major contribution
370.2	0.1357	H-9 → LUMO (94%)
515.9	0.0568	H-6 → LUMO (98%)
865.8	0.8646	HOMO → LUMO (93%)

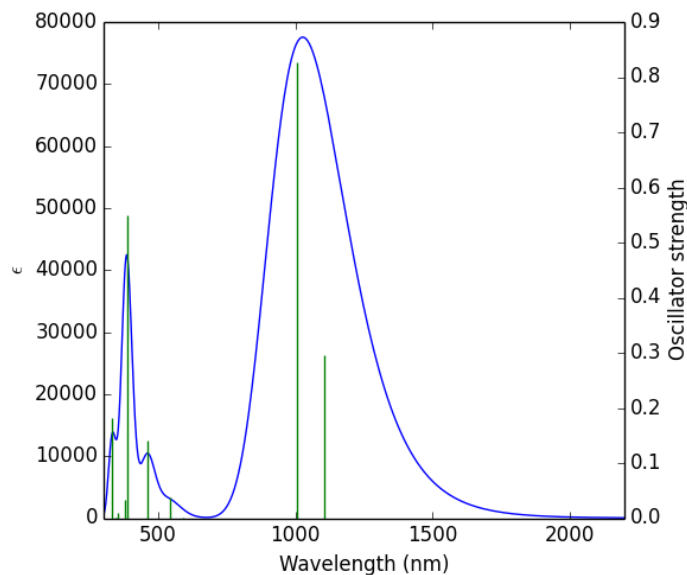


Fig. S15 TD DFT simulated spectrum of **OZ-2N**.

Table S4 Selected TD-DFT (rB3LYP/8-31G) calculated energies, oscillator strength and compositions of major electronic transitions of **OZ-2N**.

Wavelength (nm)	Oscillator strength	Major contribution
386.1	0.5504	H-1 → L+1 (94%)
462.1	0.1409	H-9 → LUMO (93%)
1004.3	0.8279	HOMO → LUMO (74%)

4. X-ray crystallographic analysis

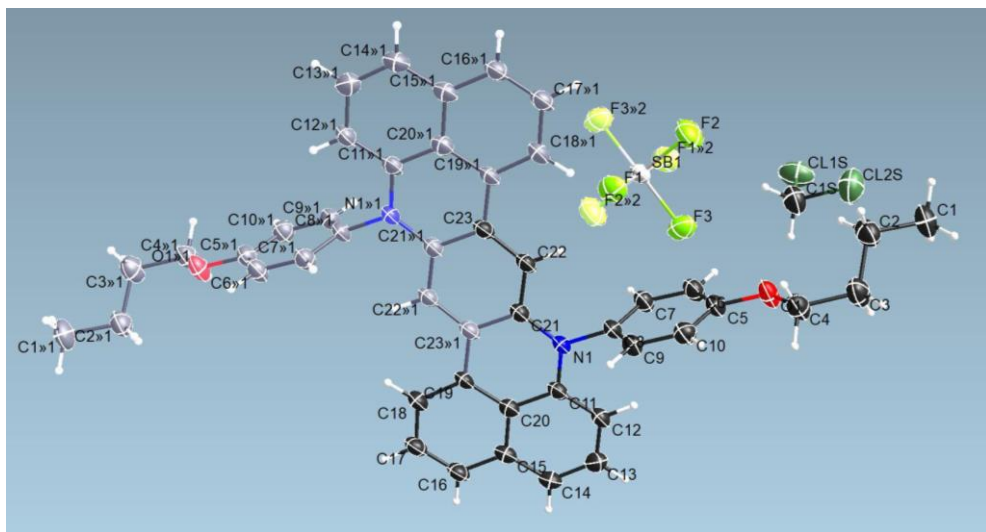


Fig. S16 ORTEP plot of dichloromethane solvate of for $7\mathbf{a}^{\bullet+}$ moiety and SbF_6^- which lies about an inversion centre. Additional characters “>>1” and “>>2” in atom labels indicate atoms generated by a centre of inversion at equivalent positions ($1-x, 2-y, 2-z$) and ($1-x, 2-y, 1-z$) respectively. Ellipsoids are drawn at the 50% probability level.

Table S5 Crystal data and structure refinement for $7\mathbf{a}^{\bullet+}$.

Empirical formula	$\text{C}_{48}\text{H}_{44}\text{Cl}_4\text{F}_6\text{N}_2\text{O}_2\text{Sb}$		
Formula weight	1058.40		
Temperature	100(2) K		
Wavelength	1.54178 Å		
Crystal system	Triclinic		
Space group	P-1		
Unit cell dimensions	$a = 8.3753(6)$ Å	$a = 87.379(3)^\circ$.	
	$b = 11.1259(9)$ Å	$b = 86.613(3)^\circ$.	
	$c = 12.1940(9)$ Å	$g = 76.612(3)^\circ$.	
Volume	$1102.86(14)$ Å ³		
Z	1		
Density (calculated)	1.594 Mg/m ³		
Absorption coefficient	7.775 mm ⁻¹		
F(000)	535		
Crystal size	0.247 x 0.200 x 0.117 mm ³		
Theta range for data collection	3.633 to 65.405°.		
Index ranges	$-9 \leq h \leq 9, -13 \leq k \leq 13, -14 \leq l \leq 12$		
Reflections collected	8771		
Independent reflections	3686 [R(int) = 0.0524]		
Completeness to theta = 65.405°	97.5 %		
Absorption correction	Semi-empirical from equivalents		

Max. and min. transmission	0.7526 and 0.3558
Refinement method	Full-matrix least-squares on F^2
Data / restraints / parameters	3686 / 0 / 287
Goodness-of-fit on F^2	1.065
Final R indices [$I > 2\sigma(I)$]	$R_1 = 0.0698$, $wR_2 = 0.1935$
R indices (all data)	$R_1 = 0.0710$, $wR_2 = 0.1956$
Extinction coefficient	n/a
Largest diff. peak and hole	2.730 and -1.310 e. \AA^{-3}

Table S6 Bond lengths [\AA] and error values of X-ray crystal structure for **7a^{•+}**.

Bond	Bond Lengths (error values)
Sb(1)-F(2)	1.867(4)
Sb(1)-F(2)#1	1.867(4)
Sb(1)-F(1)	1.868(4)
Sb(1)-F(1)#1	1.868(4)
Sb(1)-F(3)	1.870(4)
Sb(1)-F(3)#1	1.870(4)
O(1)-C(5)	1.367(7)
O(1)-C(4)	1.444(8)
N(1)-C(21)	1.376(8)
N(1)-C(11)	1.397(7)
N(1)-C(8)	1.447(7)
C(1)-C(2)	1.521(9)
C(1)-H(1A)	0.98
C(1)-H(1B)	0.98
C(1)-H(1C)	0.98
C(2)-C(3)	1.506(10)
C(2)-H(2A)	0.99
C(2)-H(2B)	0.99
C(3)-C(4)	1.522(9)
C(3)-H(3A)	0.99
C(3)-H(3B)	0.99
C(4)-H(4A)	0.99
C(4)-H(4B)	0.99
C(5)-C(10)	1.383(9)
C(5)-C(6)	1.402(9)
C(6)-C(7)	1.366(9)
C(6)-H(6)	0.95

C(7)-C(8)	1.394(8)
C(7)-H(7)	0.95
C(8)-C(9)	1.392(8)
C(9)-C(10)	1.385(8)
C(9)-H(9)	0.95
C(10)-H(10)	0.95
C(11)-C(12)	1.388(9)
C(11)-C(20)	1.415(8)
C(12)-C(13)	1.401(9)
C(12)-H(12)	0.95
C(13)-C(14)	1.368(9)
C(13)-H(13)	0.95
C(14)-C(15)	1.431(9)
C(14)-H(14)	0.95
C(15)-C(16)	1.409(8)
C(15)-C(20)	1.427(8)
C(16)-C(17)	1.377(9)
C(16)-H(16)	0.95
C(17)-C(18)	1.393(9)
C(17)-H(17)	0.95
C(18)-C(19)	1.394(8)
C(18)-H(18)	0.95
C(19)-C(20)	1.421(8)
C(19)-C(23) ^{#2}	1.455(8)
C(21)-C(22)	1.401(8)
C(21)-C(23) ^{#2}	1.431(8)
C(22)-C(23)	1.394(8)
C(22)-H(22)	0.95
Cl(1S)-C(1S)	1.769(8)
Cl(2S)-C(1S)	1.752(8)
C(1S)-H(1SA)	0.99
C(1S)-H(1SB)	0.99

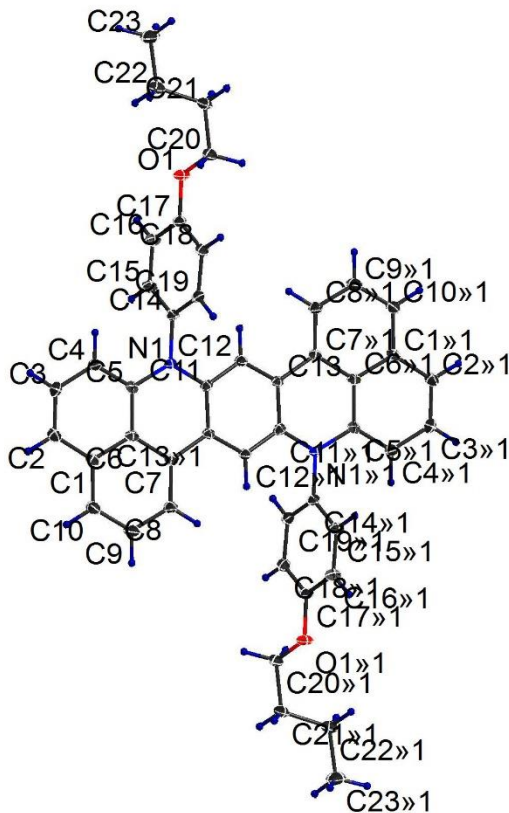


Fig. S17 ORTEP plot of **7a** which lies about an inversion centre. Additional character “>>1” in atom labels indicate atoms generated by a centre of inversion at equivalent position (1-x, 2-y, 1-z). Ellipsoids are drawn at the 50% probability level.

Table S7 Crystal data and structure refinement for **7a**.

Empirical formula	$C_{46}H_{40}N_2O_2$	
Formula weight	652.80	
Temperature	100(2) K	
Wavelength	1.54178 Å	
Crystal system	Monoclinic	
Space group	C2/c	
Unit cell dimensions	$a = 20.5080(5)$ Å	$a = 90^\circ$.
	$b = 5.60600(10)$ Å	$b = 92.5770(10)^\circ$.
	$c = 28.8557(7)$ Å	$g = 90^\circ$.
Volume	$3314.12(13)$ Å ³	
Z	4	
Density (calculated)	1.308 Mg/m ³	
Absorption coefficient	0.617 mm ⁻¹	
F(000)	1384	
Crystal size	$0.259 \times 0.109 \times 0.070$ mm ³	
Theta range for data collection	4.316 to 66.594°.	

Index ranges	-24<=h<=24, -6<=k<=6, -34<=l<=33
Reflections collected	9976
Independent reflections	2859 [R(int) = 0.0409]
Completeness to theta = 66.594°	97.2 %
Absorption correction	Semi-empirical from equivalents
Max. and min. transmission	0.7533 and 0.4366
Refinement method	Full-matrix least-squares on F ²
Data / restraints / parameters	2859 / 0 / 227
Goodness-of-fit on F ²	1.092
Final R indices [I>2sigma(I)]	R1 = 0.0391, wR2 = 0.1112
R indices (all data)	R1 = 0.0481, wR2 = 0.1281
Extinction coefficient	n/a
Largest diff. peak and hole	0.252 and -0.265 e.Å ⁻³

Table S8 Bond lengths [Å] and error values of X-ray crystal structure for **7a**.

Bond	Bond Lengths (error values)
O(1)-C(17)	1.3683(16)
O(1)-C(20)	1.4361(17)
N(1)-C(5)	1.3933(18)
N(1)-C(11)	1.4007(17)
N(1)-C(14)	1.4421(16)
C(1)-C(2)	1.416(2)
C(1)-C(10)	1.4194(19)
C(1)-C(6)	1.4270(19)
C(2)-C(3)	1.3676(19)
C(2)-H(2)	0.95
C(3)-C(4)	1.404(2)
C(3)-H(3)	0.95
C(4)-C(5)	1.3854(19)
C(4)-H(4)	0.95
C(5)-C(6)	1.4325(18)
C(6)-C(7)	1.4208(19)
C(7)-C(8)	1.3886(18)
C(7)-C(13)#1	1.4686(19)
C(8)-C(9)	1.402(2)
C(8)-H(8)	0.95
C(9)-C(10)	1.367(2)
C(9)-H(9)	0.95

C(10)-H(10)	0.95
C(11)-C(12)	1.392(2)
C(11)-C(13)#1	1.4138(18)
C(12)-C(13)	1.3930(19)
C(12)-H(12)	0.95
C(13)-C(11)#1	1.4137(18)
C(13)-C(7)#1	1.4687(19)
C(14)-C(19)	1.3772(19)
C(14)-C(15)	1.391(2)
C(15)-C(16)	1.3844(19)
C(15)-H(15)	0.95
C(16)-C(17)	1.3922(19)
C(16)-H(16)	0.95
C(17)-C(18)	1.392(2)
C(18)-C(19)	1.3951(19)
C(18)-H(18)	0.95
C(19)-H(19)	0.95
C(20)-C(21)	1.5163(18)
C(20)-H(20A)	0.99
C(20)-H(20B)	0.99
C(21)-C(22)	1.519(2)
C(21)-H(21A)	0.99
C(21)-H(21B)	0.99
C(22)-C(23)	1.5225(19)
C(22)-H(22A)	0.99
C(22)-H(22B)	0.99
C(23)-H(23A)	0.98
C(23)-H(23B)	0.98
C(23)-H(23C)	0.98

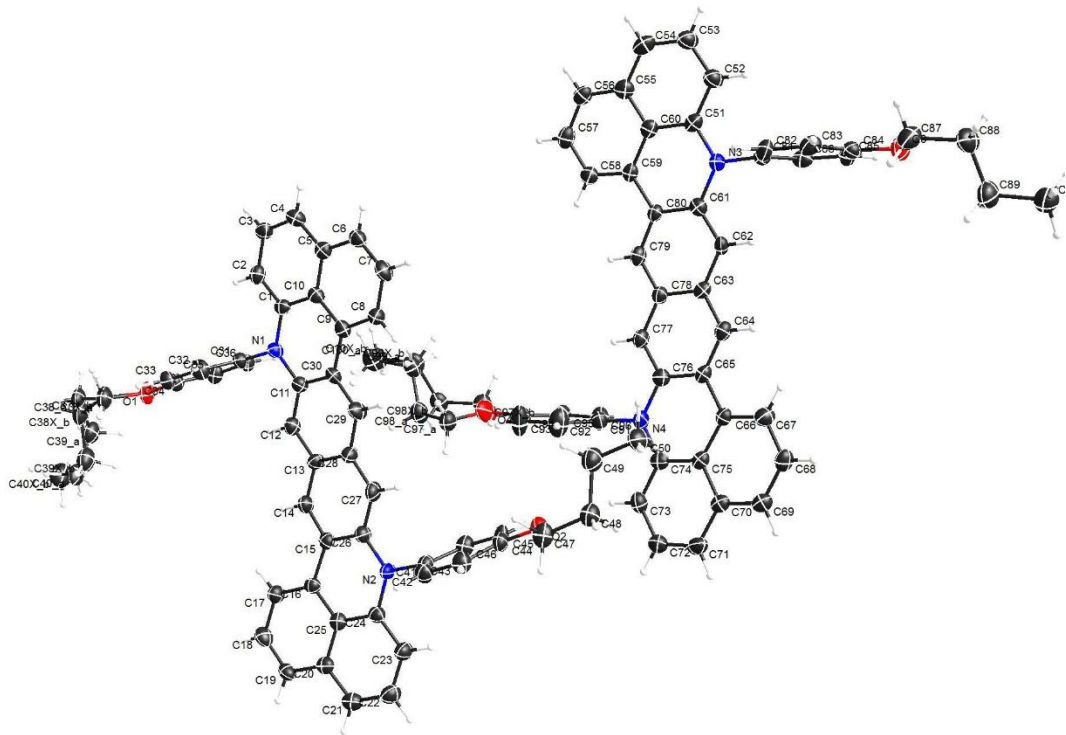


Fig. S18 ORTEP plot of the asymmetrical unit showing two molecules of **7b**. Ellipsoids are drawn at the 50% probability level. Both molecules have minor disorder component of a terminal *n*-butyl group.

Table S9 Crystal data and structure refinement for **7b**.

Empirical formula	C ₅₀ H ₄₂ N ₂ O ₂		
Formula weight	702.85		
Temperature	100(2) K		
Wavelength	1.54178 Å		
Crystal system	Orthorhombic		
Space group	P2 ₁ 2 ₁ 2 ₁		
Unit cell dimensions	a = 15.9666(5) Å	α = 90°.	
	b = 16.6567(5) Å	β = 90°.	
	c = 26.8159(9) Å	γ = 90°.	
Volume	7131.7(4) Å ³		
Z	8		
Density (calculated)	1.309 Mg/m ³		
Absorption coefficient	0.614 mm ⁻¹		
F(000)	2976		
Crystal size	0.180 x 0.113 x 0.065 mm ³		
Theta range for data collection	3.123 to 66.587°.		
Index ranges	-17<=h<=19, -13<=k<=19, -31<=l<=31		

Reflections collected	42227
Independent reflections	12567 [R(int) = 0.1130]
Completeness to theta = 66.587°	99.9 %
Absorption correction	Semi-empirical from equivalents
Max. and min. transmission	0.7533 and 0.6114
Refinement method	Full-matrix least-squares on F ²
Data / restraints / parameters	12567 / 238 / 1053
Goodness-of-fit on F ²	0.983
Final R indices [I>2sigma(I)]	R1 = 0.0580, wR2 = 0.1223
R indices (all data)	R1 = 0.1277, wR2 = 0.1587
Absolute structure parameter	-0.4(4)
Extinction coefficient	n/a
Largest diff. peak and hole	0.263 and -0.301 e.Å ⁻³

Table S10 Bond lengths [Å] and error values of X-ray crystal structure for **7b**.

Bond	Bond Lengths (error values)
C(37)-O(1)	1.438(9)
C(37)-C(38)	1.521(11)
C(37)-H(37A)	0.99
C(37)-H(37B)	0.99
C(38)-C(39)	1.516(11)
C(38)-H(38A)	0.99
C(38)-H(38B)	0.99
C(39)-C(40)	1.525(10)
C(39)-H(39A)	0.99
C(39)-H(39B)	0.99
C(40)-H(40A)	0.98
C(40)-H(40B)	0.98
C(40)-H(40C)	0.98
C(97)-O(4)	1.250(10)
C(97)-C(98)	1.505(10)
C(97)-H(97A)	0.99
C(97)-H(97B)	0.99
C(98)-C(99)	1.500(11)
C(98)-H(98A)	0.99
C(98)-H(98B)	0.99
C(99)-C(100)	1.495(10)
C(99)-H(99A)	0.99

C(99)-H(99B)	0.99
C(100)-H(10A)	0.98
C(100)-H(10B)	0.98
C(100)-H(10C)	0.98
C(37X)-O(1)	1.437(11)
C(37X)-C(38X)	1.520(10)
C(37X)-H(37C)	0.99
C(37X)-H(37D)	0.99
C(38X)-C(39X)	1.523(11)
C(38X)-H(38C)	0.99
C(38X)-H(38D)	0.99
C(39X)-C(40X)	1.528(11)
C(39X)-H(39C)	0.99
C(39X)-H(39D)	0.99
C(40X)-H(40D)	0.98
C(40X)-H(40E)	0.98
C(40X)-H(40F)	0.98
C(97X)-O(4)	1.260(10)
C(97X)-C(98X)	1.490(9)
C(97X)-H(97C)	0.99
C(97X)-H(97D)	0.99
C(98X)-C(99X)	1.502(10)
C(98X)-H(98C)	0.99
C(98X)-H(98D)	0.99
C(99X)-C(10X)	1.500(10)
C(99X)-H(99C)	0.99
C(99X)-H(99D)	0.99
C(10X)-H(10D)	0.98
C(10X)-H(10E)	0.98
C(10X)-H(10F)	0.98
O(1)-C(34)	1.365(7)
O(2)-C(44)	1.380(7)
O(2)-C(47)	1.432(7)
O(3)-C(84)	1.370(7)
O(3)-C(87)	1.442(7)
O(4)-C(94)	1.363(7)
N(1)-C(11)	1.406(7)
N(1)-C(1)	1.408(7)

N(1)-C(31)	1.438(7)
N(2)-C(24)	1.399(7)
N(2)-C(26)	1.403(7)
N(2)-C(41)	1.443(8)
N(3)-C(51)	1.399(7)
N(3)-C(61)	1.399(7)
N(3)-C(81)	1.442(7)
N(4)-C(76)	1.400(7)
N(4)-C(74)	1.403(7)
N(4)-C(91)	1.447(8)
C(1)-C(2)	1.377(8)
C(1)-C(10)	1.429(8)
C(2)-C(3)	1.399(8)
C(2)-H(2)	0.95
C(3)-C(4)	1.354(8)
C(3)-H(3)	0.95
C(4)-C(5)	1.429(8)
C(4)-H(4)	0.95
C(5)-C(10)	1.414(8)
C(5)-C(6)	1.418(8)
C(6)-C(7)	1.346(8)
C(6)-H(6)	0.95
C(7)-C(8)	1.404(8)
C(7)-H(7)	0.95
C(8)-C(9)	1.385(8)
C(8)-H(8)	0.95
C(9)-C(10)	1.425(8)
C(9)-C(30)	1.482(8)
C(11)-C(12)	1.382(8)
C(11)-C(30)	1.413(8)
C(12)-C(13)	1.402(8)
C(12)-H(12)	0.95
C(13)-C(14)	1.409(8)
C(13)-C(28)	1.422(8)
C(14)-C(15)	1.389(8)
C(14)-H(14)	0.95
C(15)-C(26)	1.424(8)
C(15)-C(16)	1.476(8)

C(16)-C(17)	1.375(8)
C(16)-C(25)	1.424(8)
C(17)-C(18)	1.397(8)
C(17)-H(17)	0.95
C(18)-C(19)	1.365(8)
C(18)-H(18)	0.95
C(19)-C(20)	1.417(8)
C(19)-H(19)	0.95
C(20)-C(21)	1.415(8)
C(20)-C(25)	1.425(8)
C(21)-C(22)	1.355(9)
C(21)-H(21)	0.95
C(22)-C(23)	1.396(8)
C(22)-H(22)	0.95
C(23)-C(24)	1.391(8)
C(23)-H(23)	0.95
C(24)-C(25)	1.423(8)
C(26)-C(27)	1.387(8)
C(27)-C(28)	1.407(8)
C(27)-H(27)	0.95
C(28)-C(29)	1.401(8)
C(29)-C(30)	1.385(8)
C(29)-H(29)	0.95
C(31)-C(32)	1.368(8)
C(31)-C(36)	1.383(8)
C(32)-C(33)	1.380(8)
C(32)-H(32)	0.95
C(33)-C(34)	1.387(8)
C(33)-H(33)	0.95
C(34)-C(35)	1.369(8)
C(35)-C(36)	1.392(8)
C(35)-H(35)	0.95
C(36)-H(36)	0.95
C(41)-C(42)	1.373(8)
C(41)-C(46)	1.386(8)
C(42)-C(43)	1.386(8)
C(42)-H(42)	0.95
C(43)-C(44)	1.380(8)

C(43)-H(43)	0.95
C(44)-C(45)	1.373(8)
C(45)-C(46)	1.376(8)
C(45)-H(45)	0.95
C(46)-H(46)	0.95
C(47)-C(48)	1.493(8)
C(47)-H(47A)	0.99
C(47)-H(47B)	0.99
C(48)-C(49)	1.516(8)
C(48)-H(48A)	0.99
C(48)-H(48B)	0.99
C(49)-C(50)	1.501(8)
C(49)-H(49A)	0.99
C(49)-H(49B)	0.99
C(50)-H(50A)	0.98
C(50)-H(50B)	0.98
C(50)-H(50C)	0.98
C(51)-C(52)	1.381(8)
C(51)-C(60)	1.426(8)
C(52)-C(53)	1.409(8)
C(52)-H(52)	0.95
C(53)-C(54)	1.366(8)
C(53)-H(53)	0.95
C(54)-C(55)	1.418(8)
C(54)-H(54)	0.95
C(55)-C(56)	1.398(8)
C(55)-C(60)	1.436(8)
C(56)-C(57)	1.371(8)
C(56)-H(56)	0.95
C(57)-C(58)	1.390(8)
C(57)-H(57)	0.95
C(58)-C(59)	1.388(8)
C(58)-H(58)	0.95
C(59)-C(60)	1.419(8)
C(59)-C(80)	1.473(7)
C(61)-C(62)	1.382(8)
C(61)-C(80)	1.432(8)
C(62)-C(63)	1.404(8)

C(62)-H(62)	0.95
C(63)-C(64)	1.418(8)
C(63)-C(78)	1.419(8)
C(64)-C(65)	1.373(8)
C(64)-H(64)	0.95
C(65)-C(76)	1.430(8)
C(65)-C(66)	1.475(8)
C(66)-C(67)	1.374(8)
C(66)-C(75)	1.441(8)
C(67)-C(68)	1.413(8)
C(67)-H(67)	0.95
C(68)-C(69)	1.360(8)
C(68)-H(68)	0.95
C(69)-C(70)	1.410(8)
C(69)-H(69)	0.95
C(70)-C(71)	1.413(8)
C(70)-C(75)	1.433(8)
C(71)-C(72)	1.369(8)
C(71)-H(71)	0.95
C(72)-C(73)	1.394(8)
C(72)-H(72)	0.95
C(73)-C(74)	1.389(8)
C(73)-H(73)	0.95
C(74)-C(75)	1.420(8)
C(76)-C(77)	1.380(8)
C(77)-C(78)	1.412(8)
C(77)-H(77)	0.95
C(78)-C(79)	1.405(8)
C(79)-C(80)	1.373(8)
C(79)-H(79)	0.95
C(81)-C(82)	1.368(8)
C(81)-C(86)	1.380(8)
C(82)-C(83)	1.402(8)
C(82)-H(82)	0.95
C(83)-C(84)	1.389(8)
C(83)-H(83)	0.95
C(84)-C(85)	1.390(8)
C(85)-C(86)	1.385(8)

C(85)-H(85)	0.95
C(86)-H(86)	0.95
C(87)-C(88)	1.507(8)
C(87)-H(87A)	0.99
C(87)-H(87B)	0.99
C(88)-C(89)	1.538(9)
C(88)-H(88A)	0.99
C(88)-H(88B)	0.99
C(89)-C(90)	1.501(8)
C(89)-H(89A)	0.99
C(89)-H(89B)	0.99
C(90)-H(90A)	0.98
C(90)-H(90B)	0.98
C(90)-H(90C)	0.98
C(91)-C(96)	1.365(8)
C(91)-C(92)	1.369(8)
C(92)-C(93)	1.395(9)
C(92)-H(92)	0.95
C(93)-C(94)	1.362(9)
C(93)-H(93)	0.95
C(94)-C(95)	1.377(8)
C(95)-C(96)	1.369(8)
C(95)-H(95)	0.95
C(96)-H(96)	0.95

5. Additional $^1\text{H}/^{13}\text{C}$ NMR and mass spectra

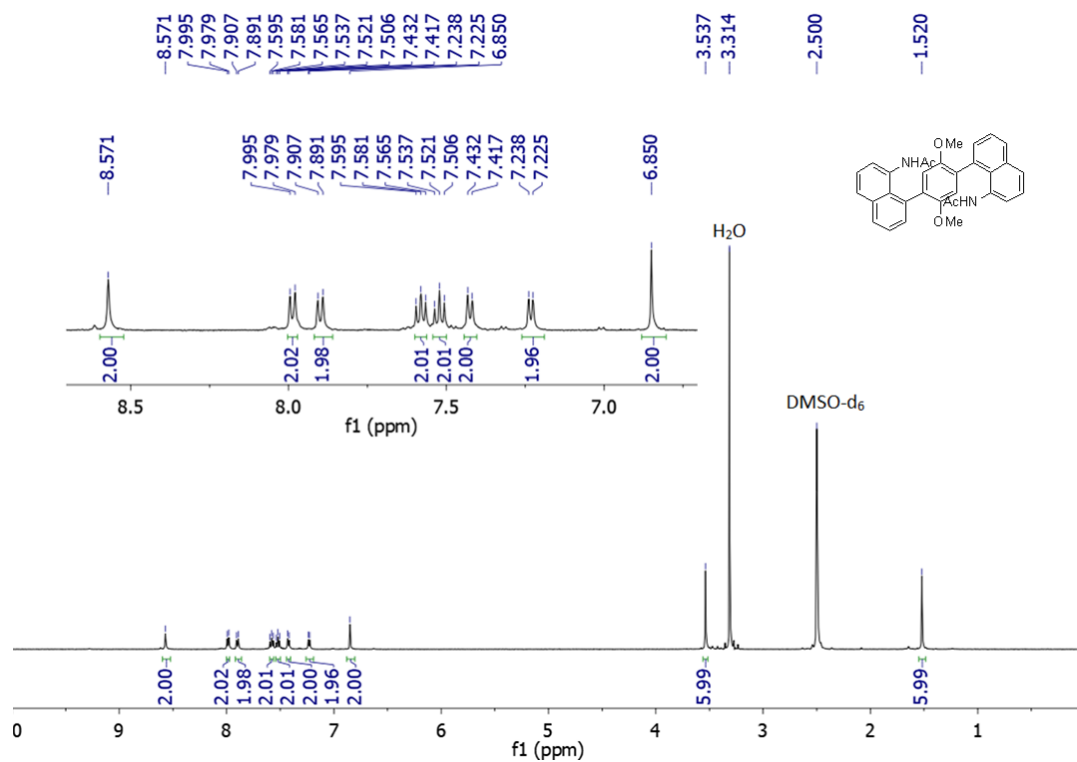


Fig. S19 ^1H NMR spectrum of **3a** (500 MHz, DMSO-d₆, rt).

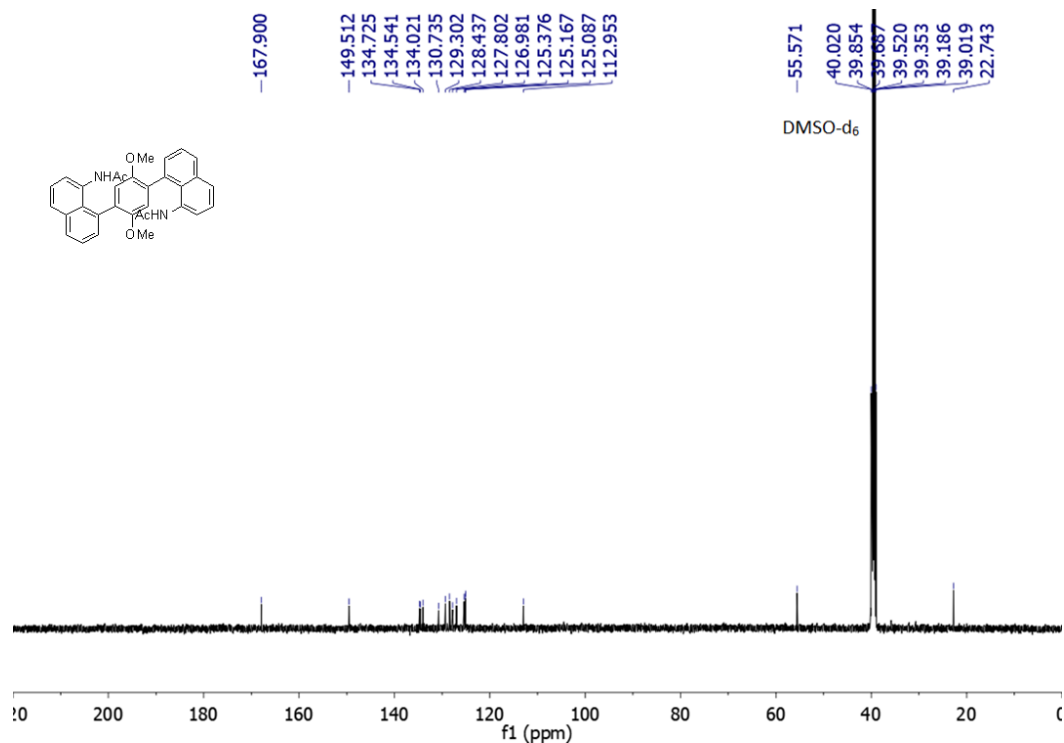


Fig. S20 ^{13}C NMR spectrum of **3a** (125 MHz, DMSO-d₆, rt).

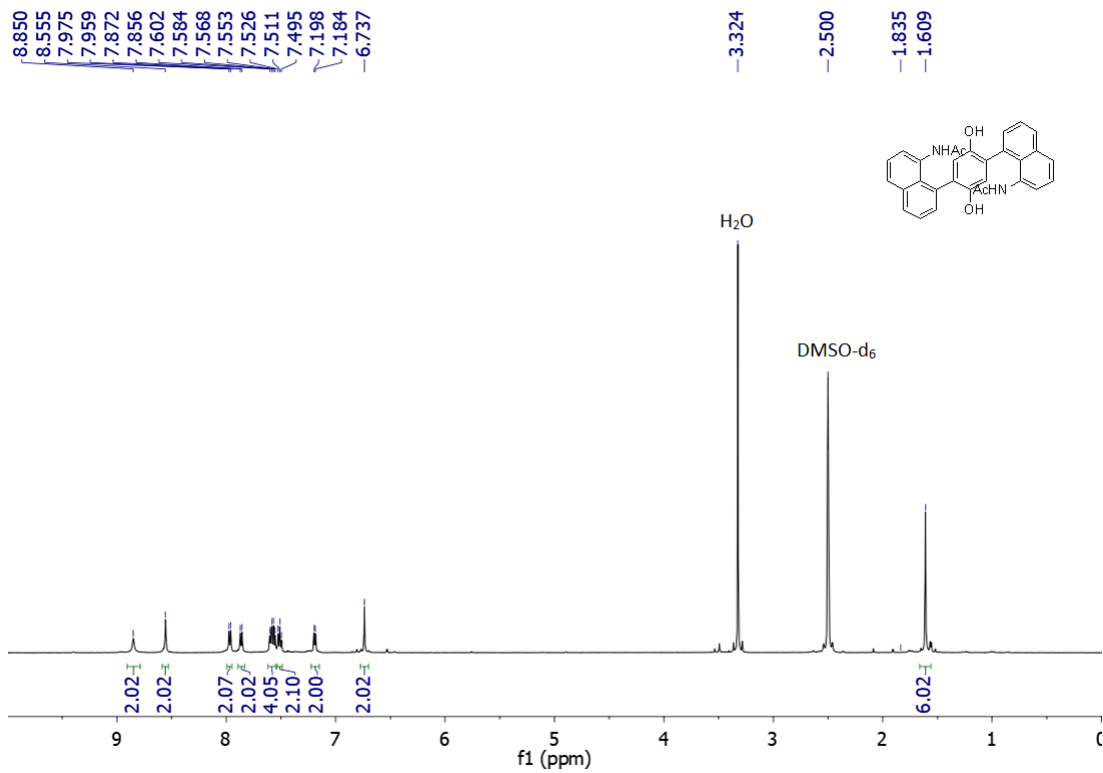


Fig. S21 ^1H NMR spectrum of **4a** (500 MHz, DMSO- d_6 , rt).

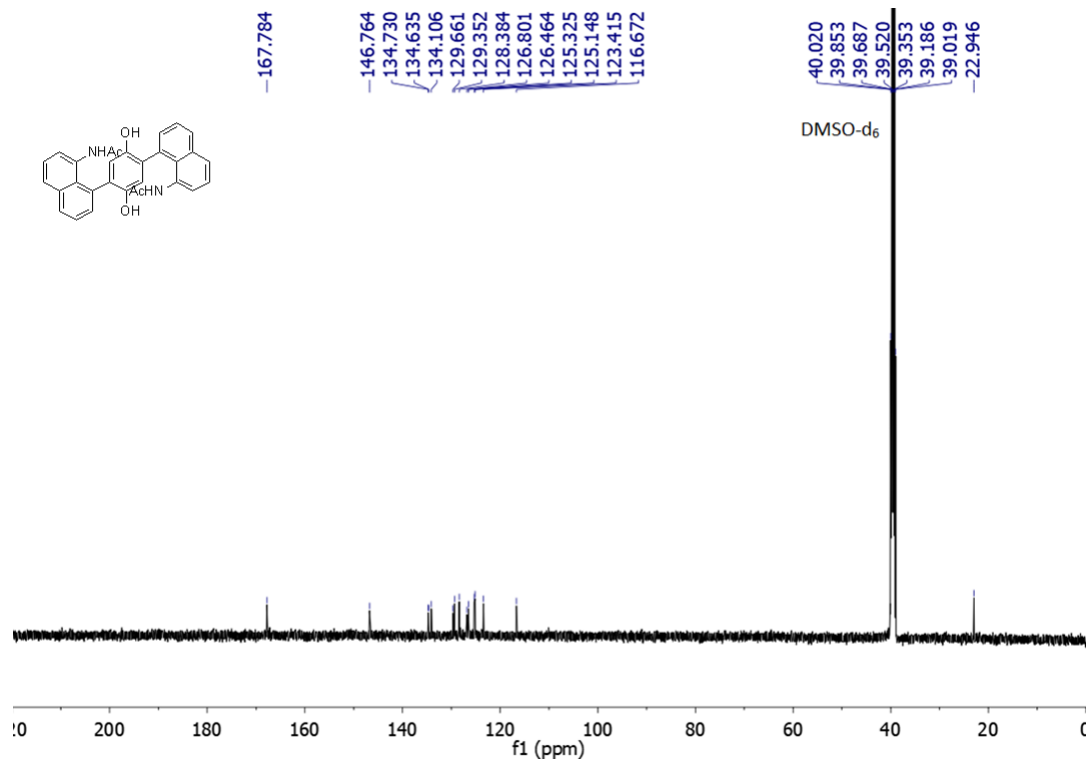


Fig. S22 ^{13}C NMR spectrum of **4a** (125 MHz, DMSO- d_6 , rt).

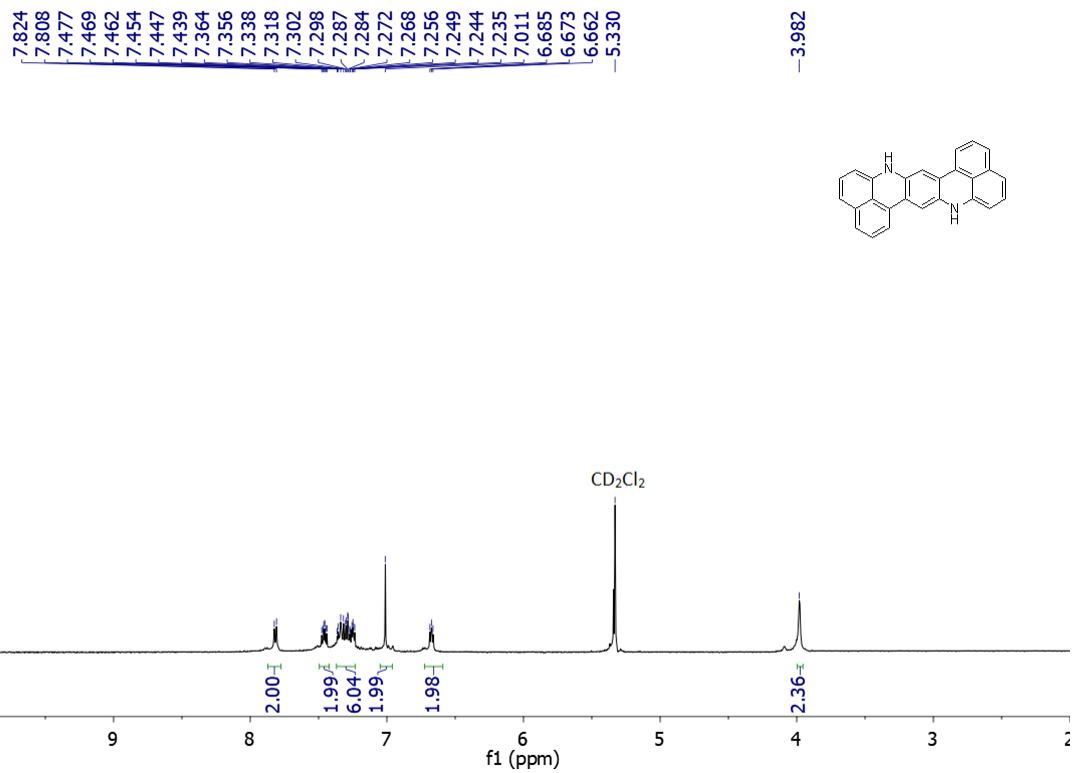


Fig. S23 ¹H NMR spectrum of **5a** (500 MHz, CD_2Cl_2 , rt).

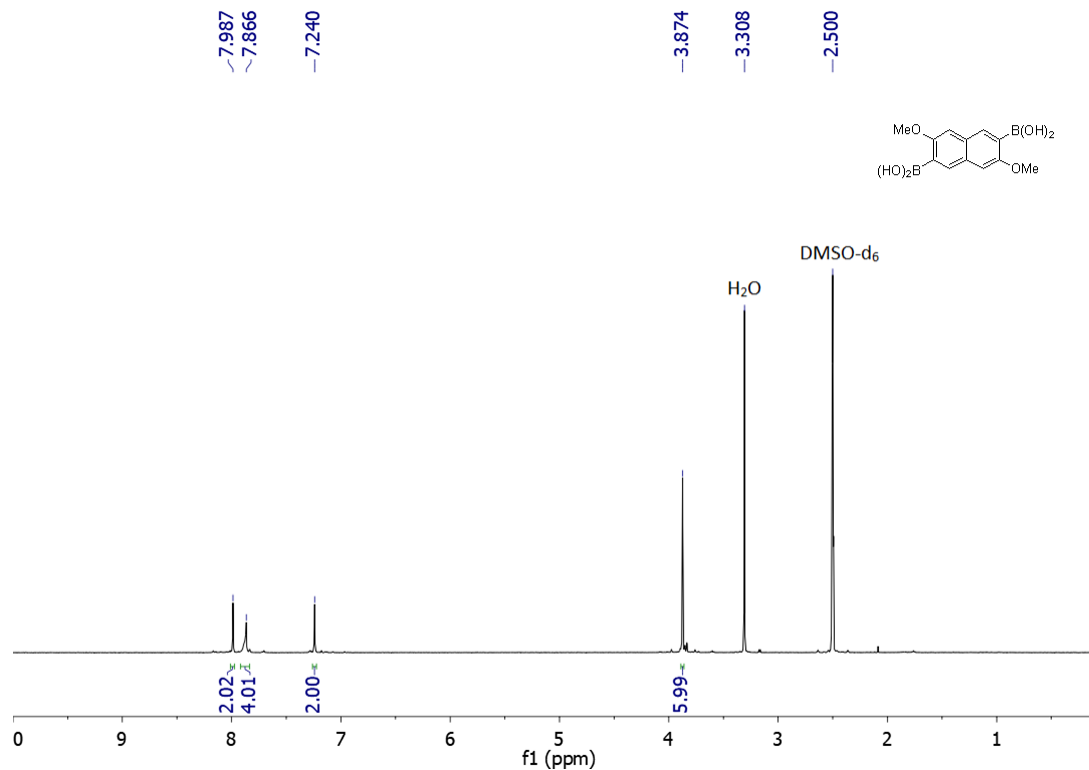


Fig. S24 ¹H NMR spectrum of **2b** (500 MHz, DMSO-d₆, rt).

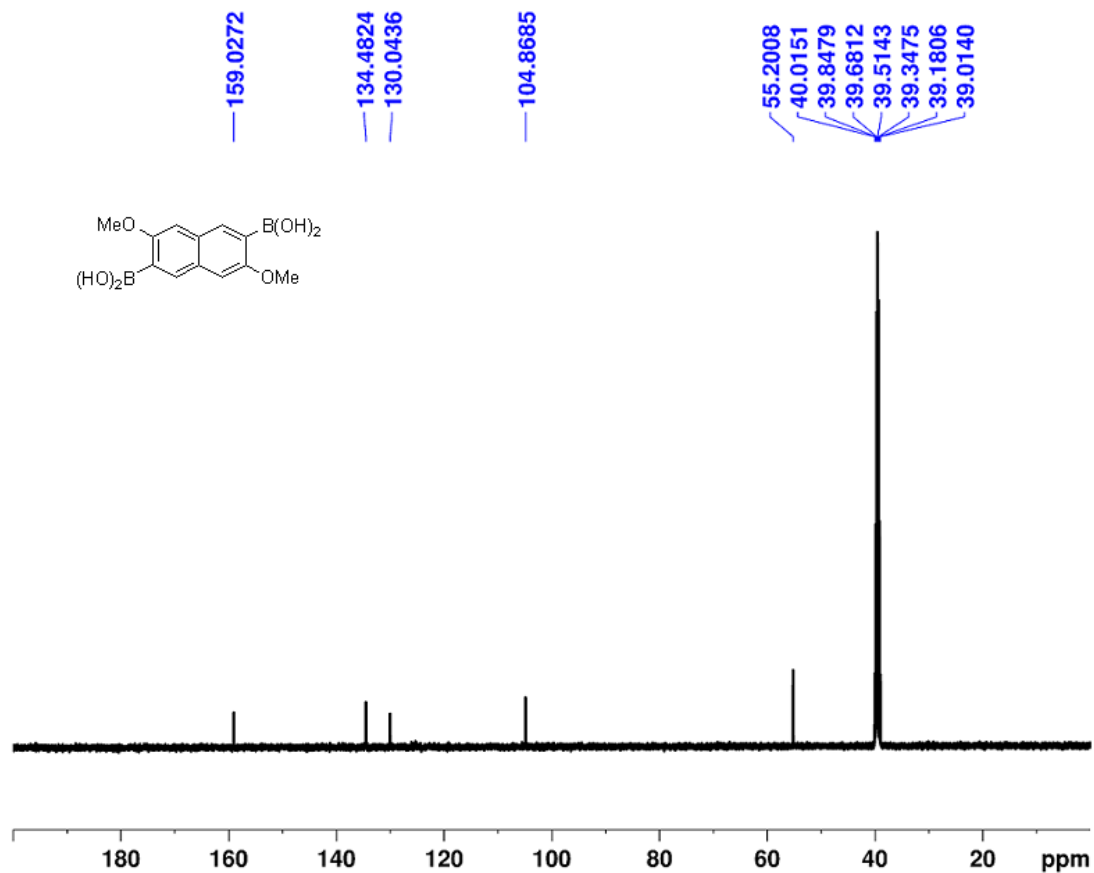


Fig. S25 ^{13}C NMR spectrum of **2b** (125 MHz, DMSO-d₆, rt).

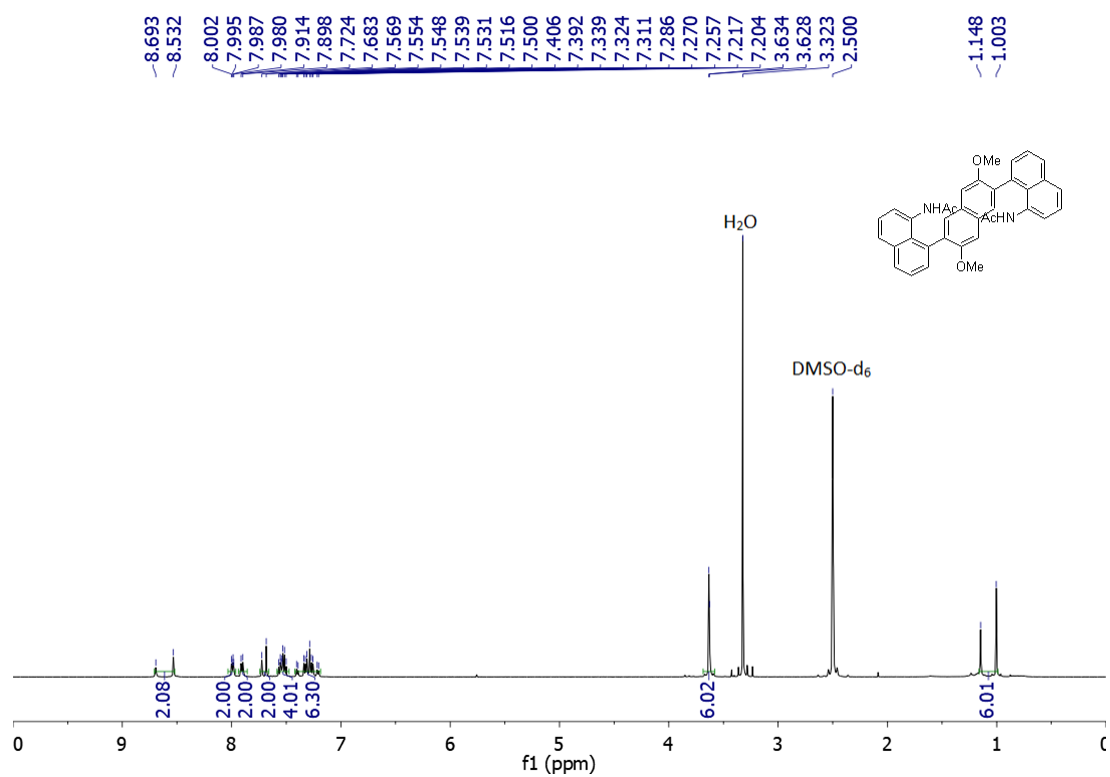


Fig. S26 ^1H NMR spectrum of **3b** (500 MHz, DMSO-d₆, rt).

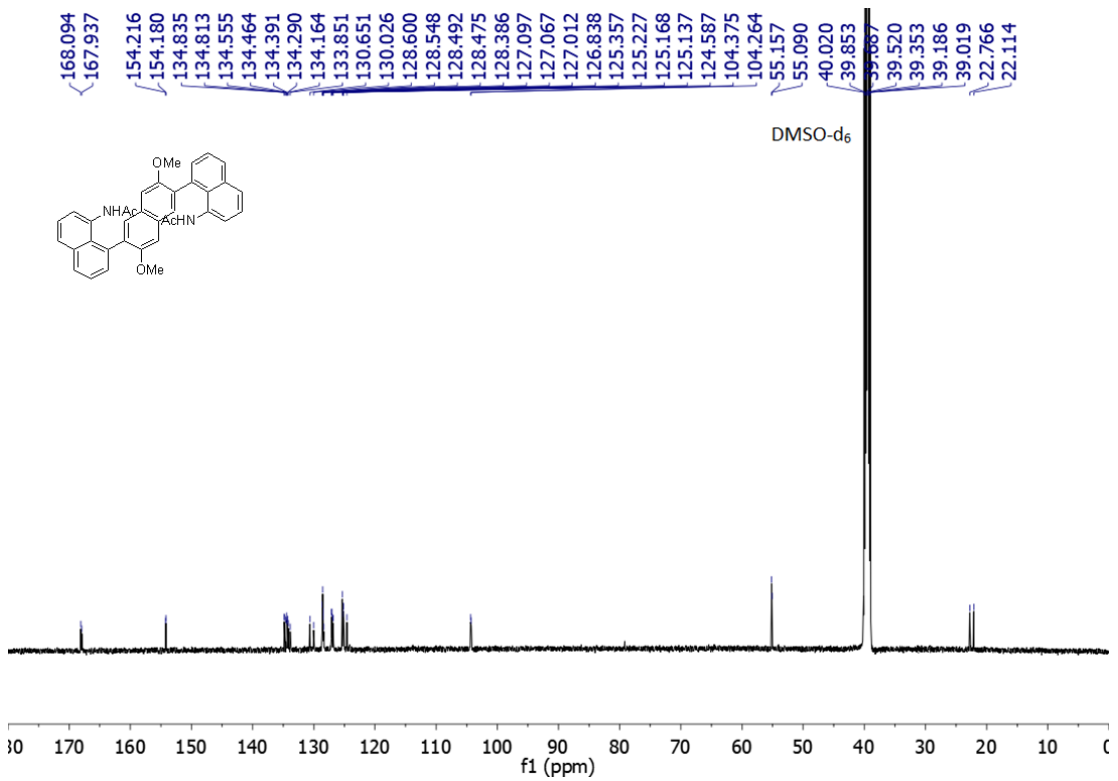


Fig. S27 ^{13}C NMR spectrum of **3b** (125 MHz, DMSO-d₆, rt).

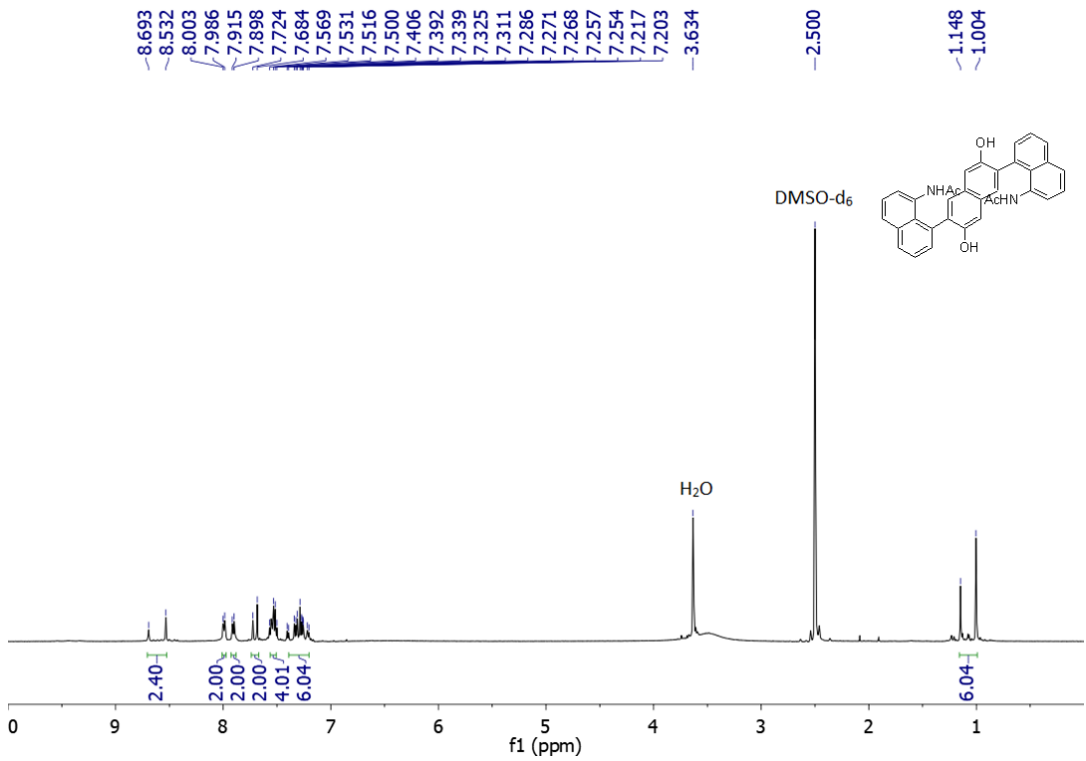


Fig. S28 ^1H NMR spectrum of **4b** (500 MHz, DMSO-d₆, rt).

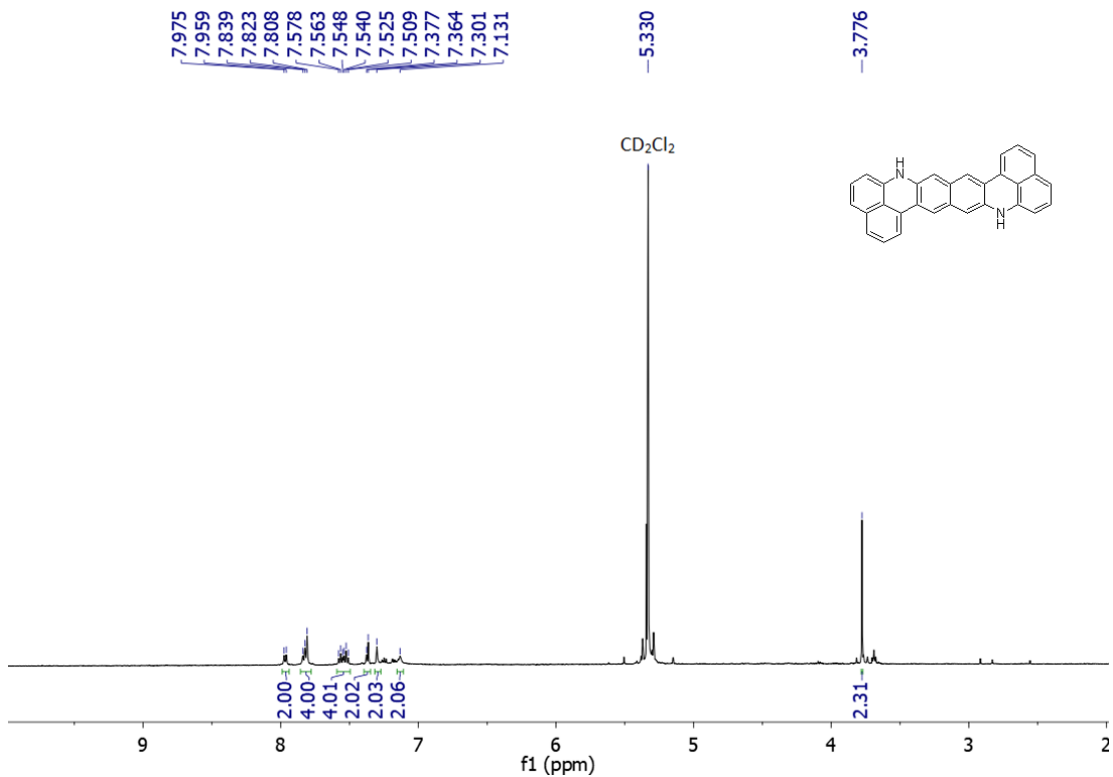


Fig. S29 ^1H NMR spectrum of **5b** (500 MHz, CD_2Cl_2 , rt).

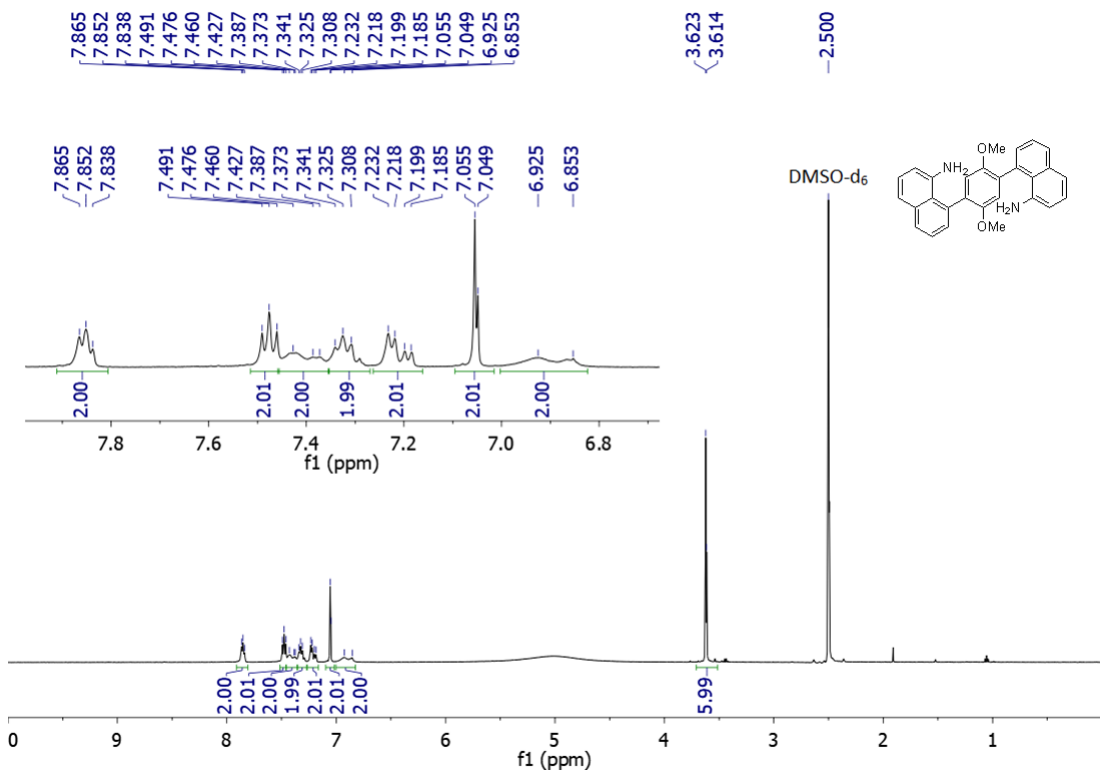


Fig. S30 ^1H NMR spectrum of **6a** (500 MHz, DMSO-d_6 , rt).

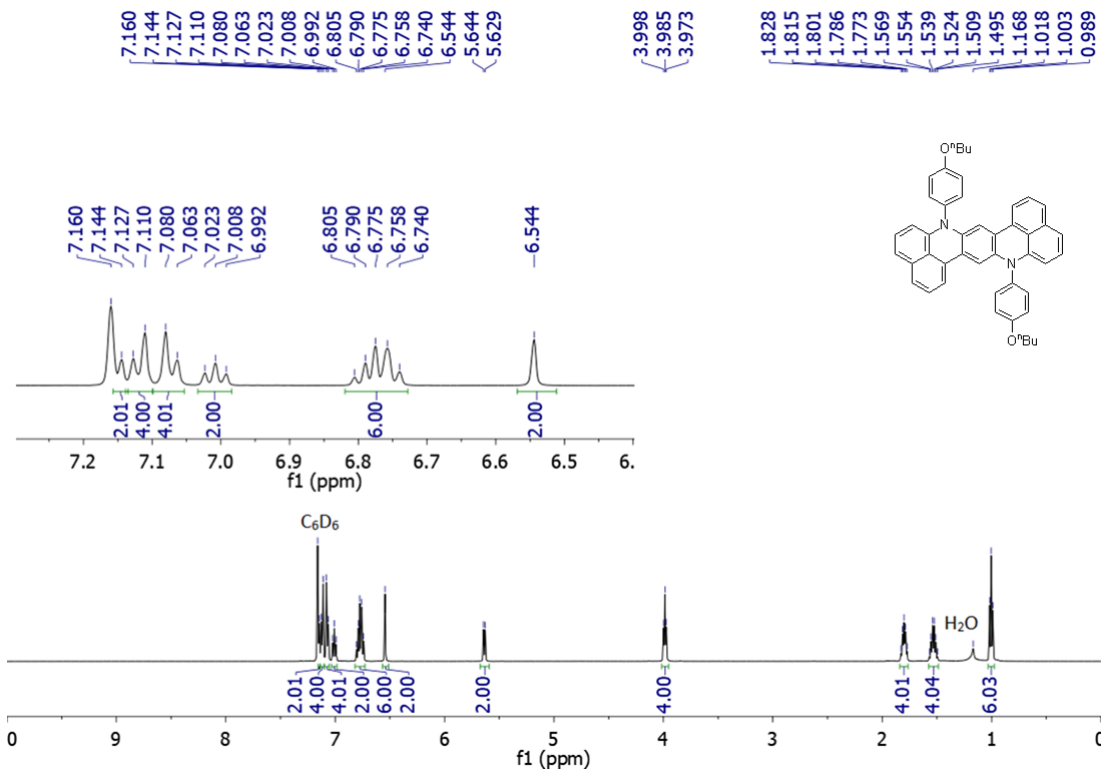


Fig. S31 ^1H NMR spectrum of **7a** (500 MHz, $\text{CS}_2/\text{C}_6\text{D}_6$, rt).

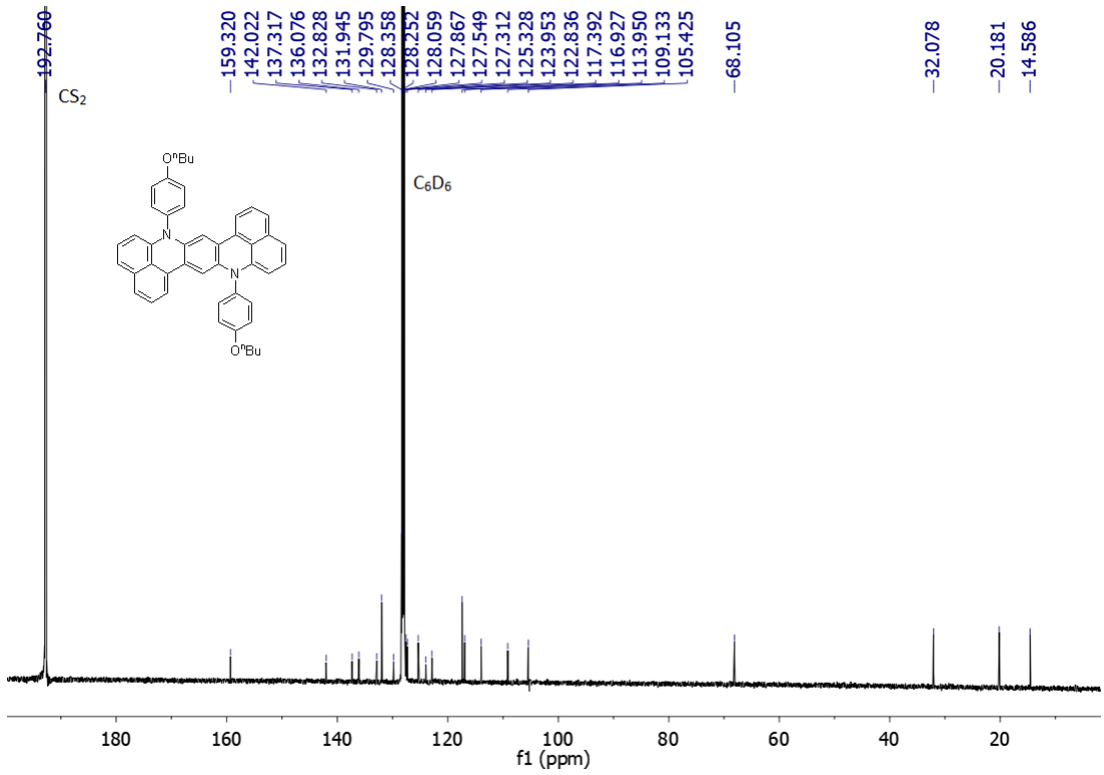


Fig. S32 ^{13}C NMR spectrum of **7a** (125 MHz, $\text{CS}_2/\text{C}_6\text{D}_6$, rt).

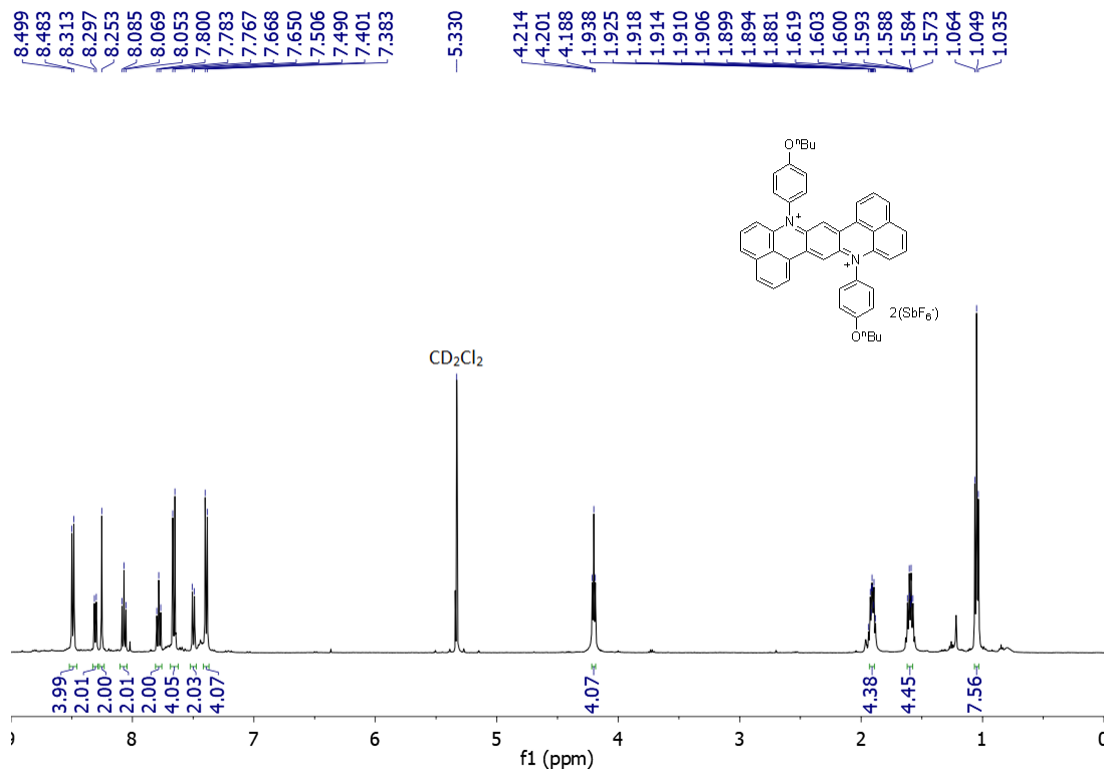


Fig. S33 ¹H NMR spectrum of **HZ-2N** (500 MHz, CD₂Cl₂, -10 °C).

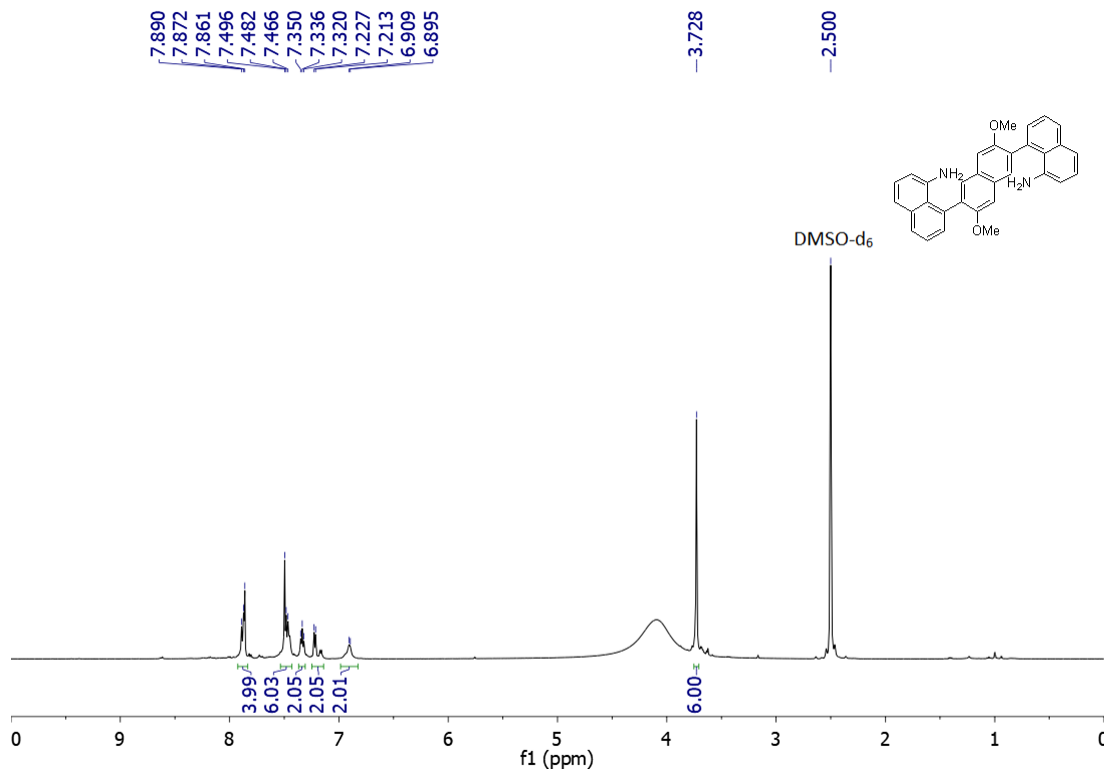


Fig. S34 ¹H NMR spectrum of **6b** (500 MHz, DMSO-d₆, rt).

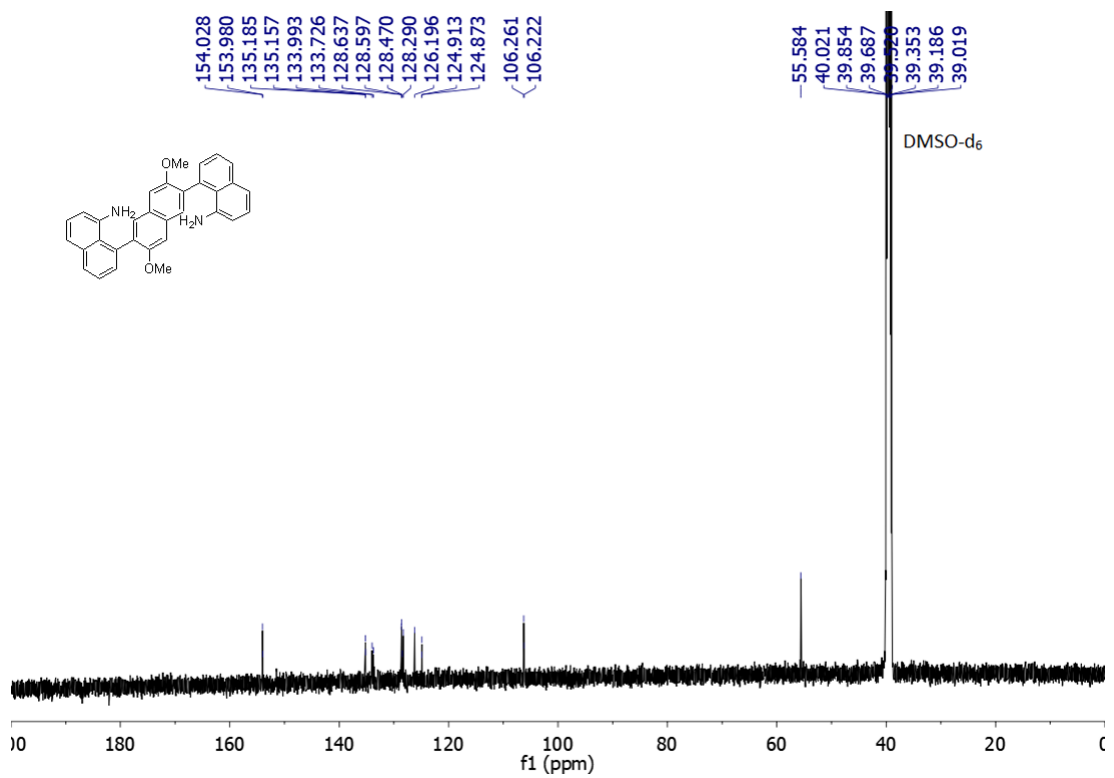


Fig. S35 ^{13}C NMR spectrum of **6b** (125 MHz, DMSO-d_6 , rt).

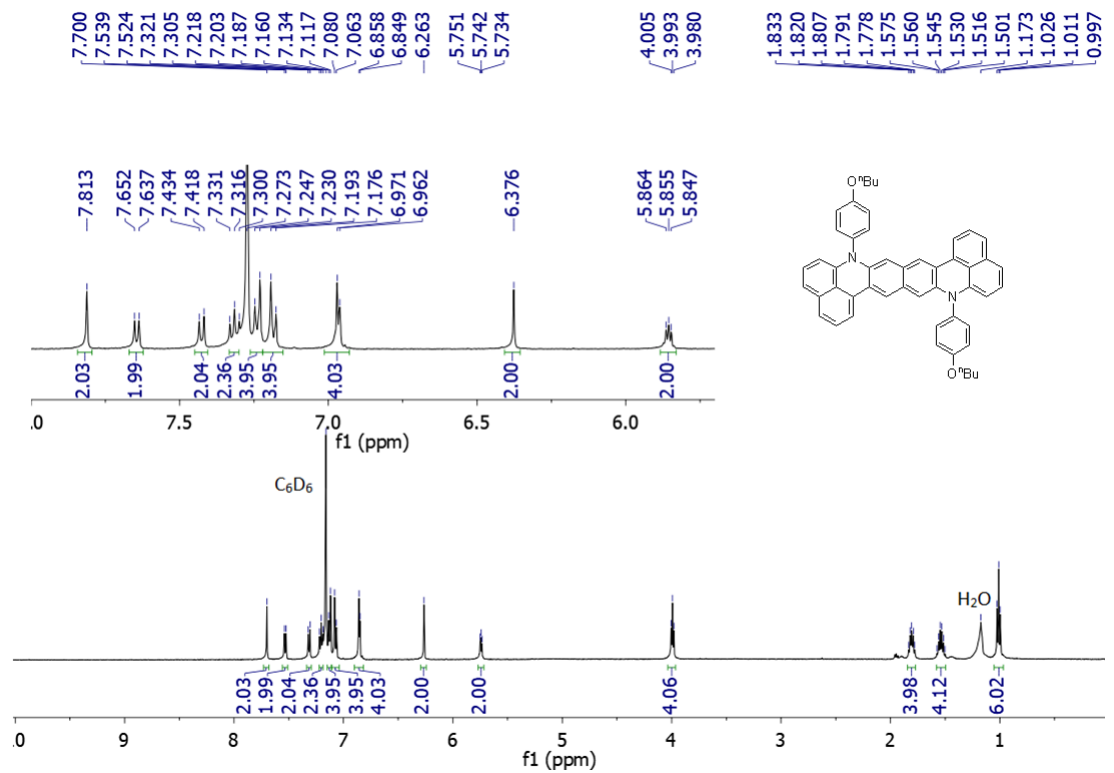


Fig. S36 ^1H NMR spectrum of **7b** (500 MHz, $\text{CS}_2/\text{C}_6\text{D}_6$, rt).

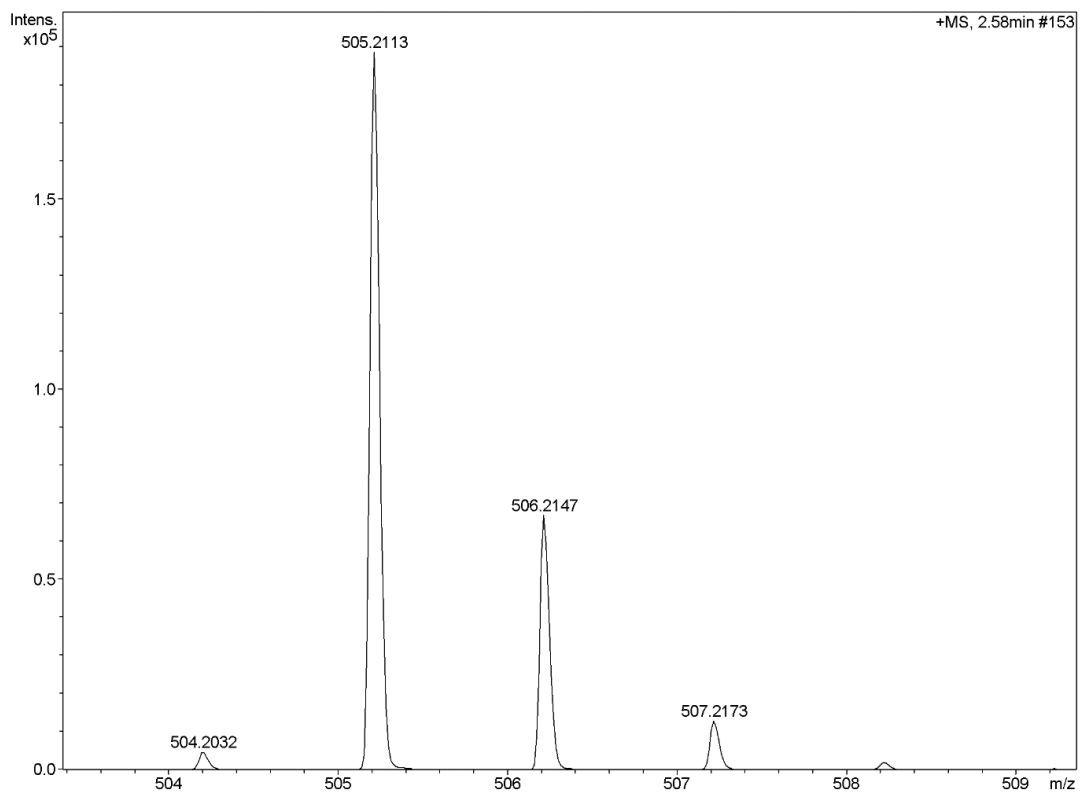


Fig. S37 HR mass spectrum (APCI) of **3a**.

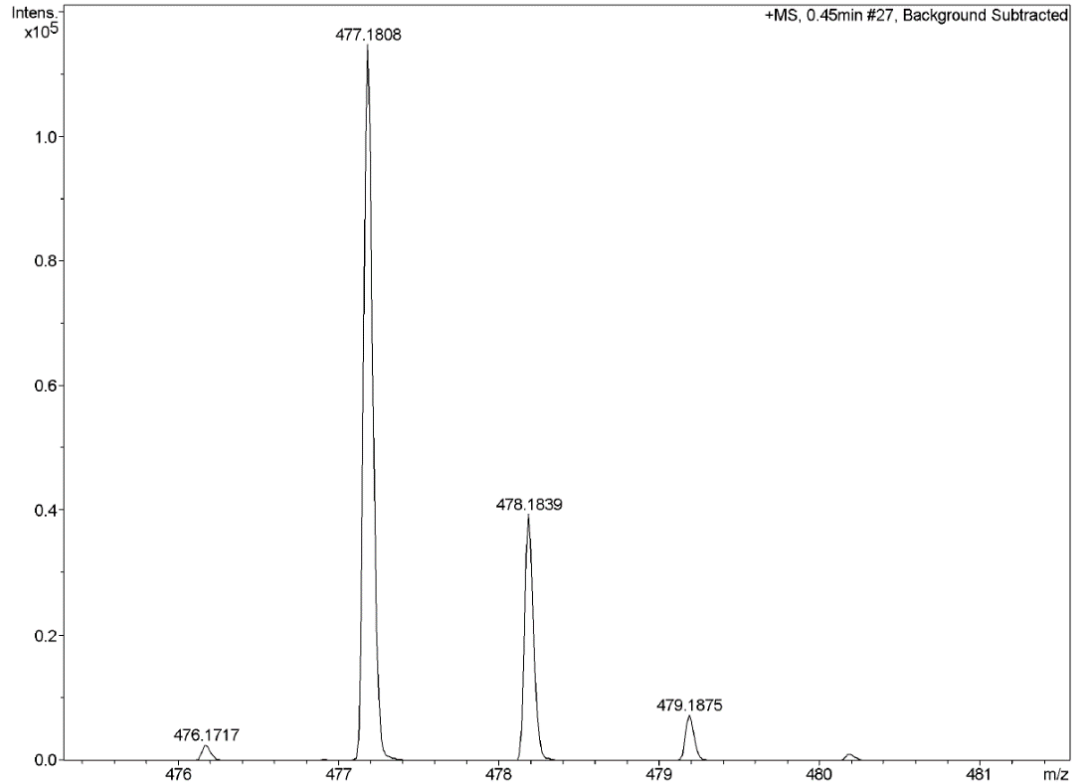


Fig. S38 HR mass spectrum (APCI) of **4a**.

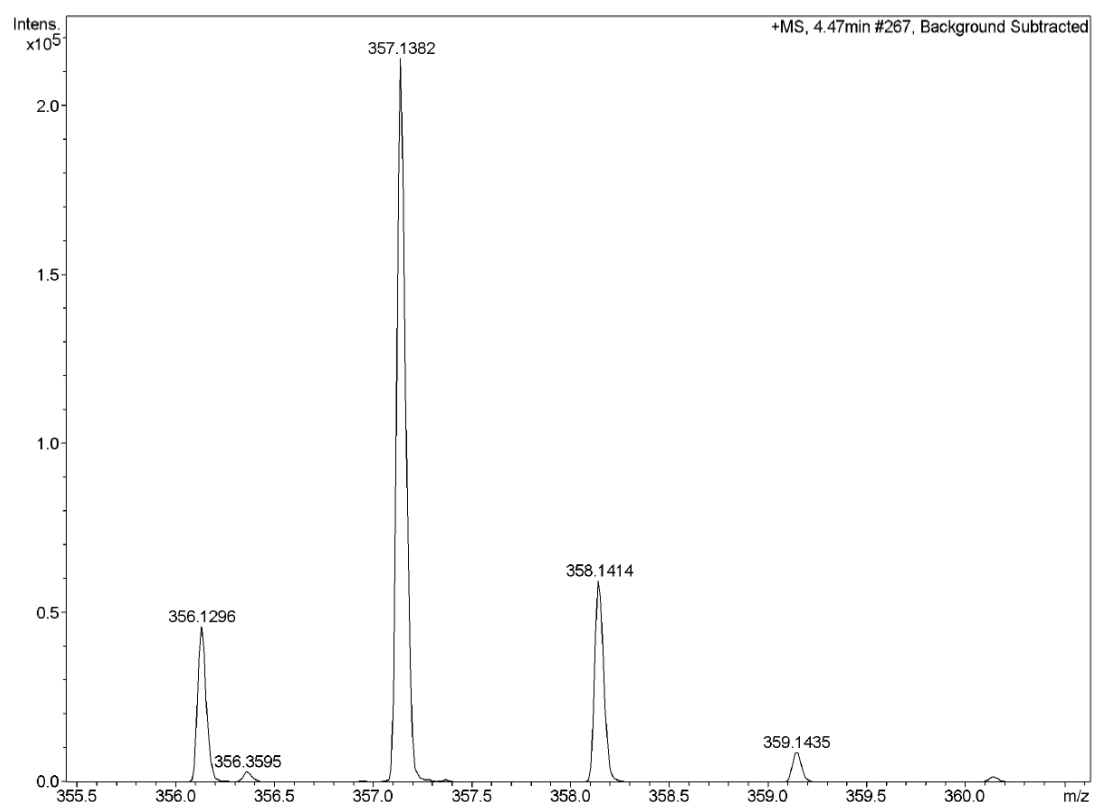


Fig. S39 HR mass spectrum (APCI) of **5a**.

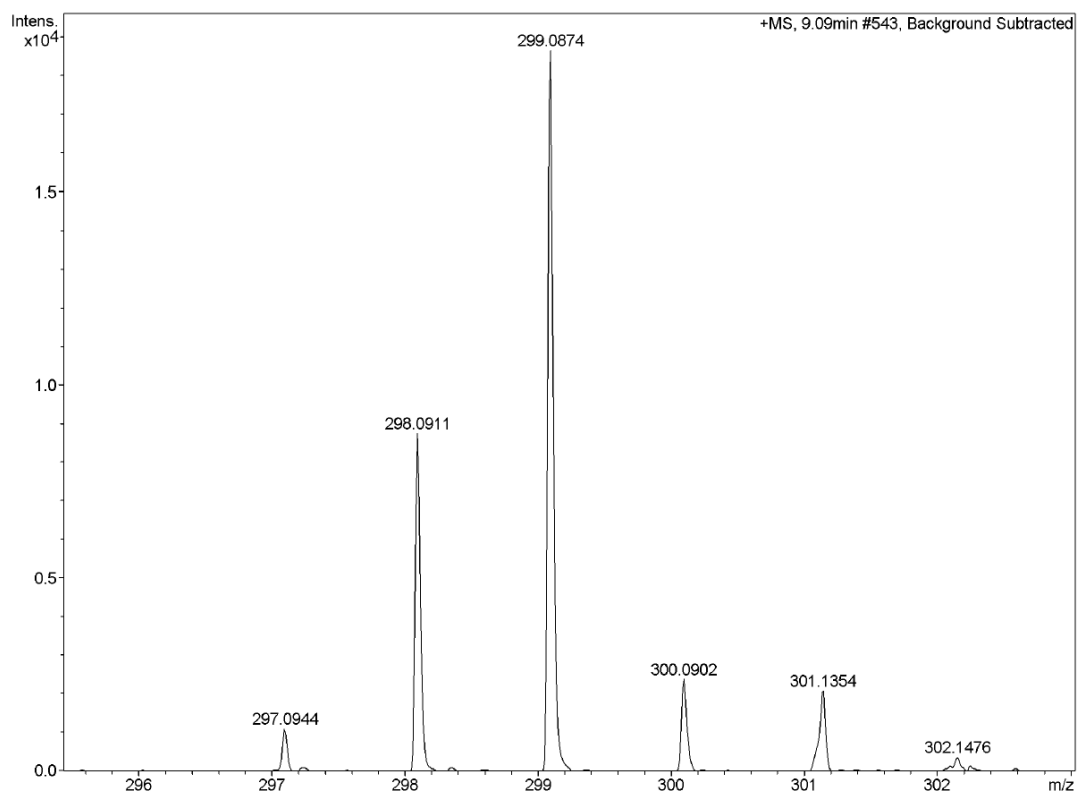


Fig. S40 HR mass spectrum (ESI) of **2b**.

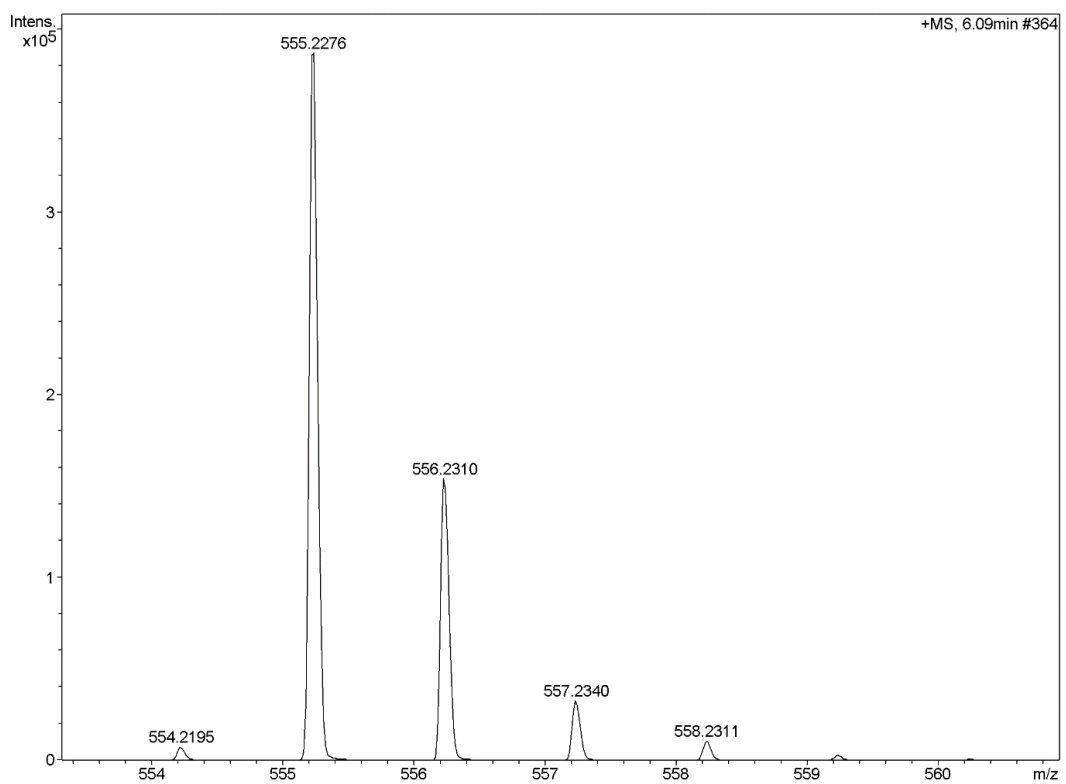


Fig. S41 HR mass spectrum (APCI) of **3b**.

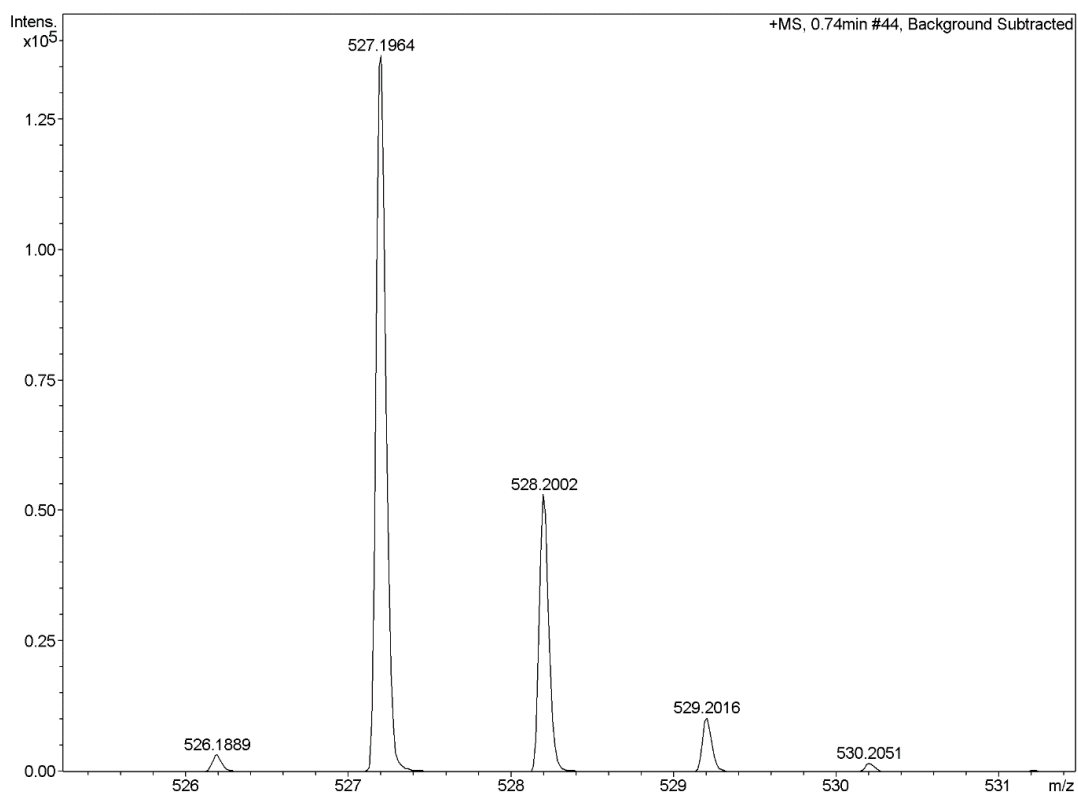


Fig. S42 HR mass spectrum (APCI) of **4b**.

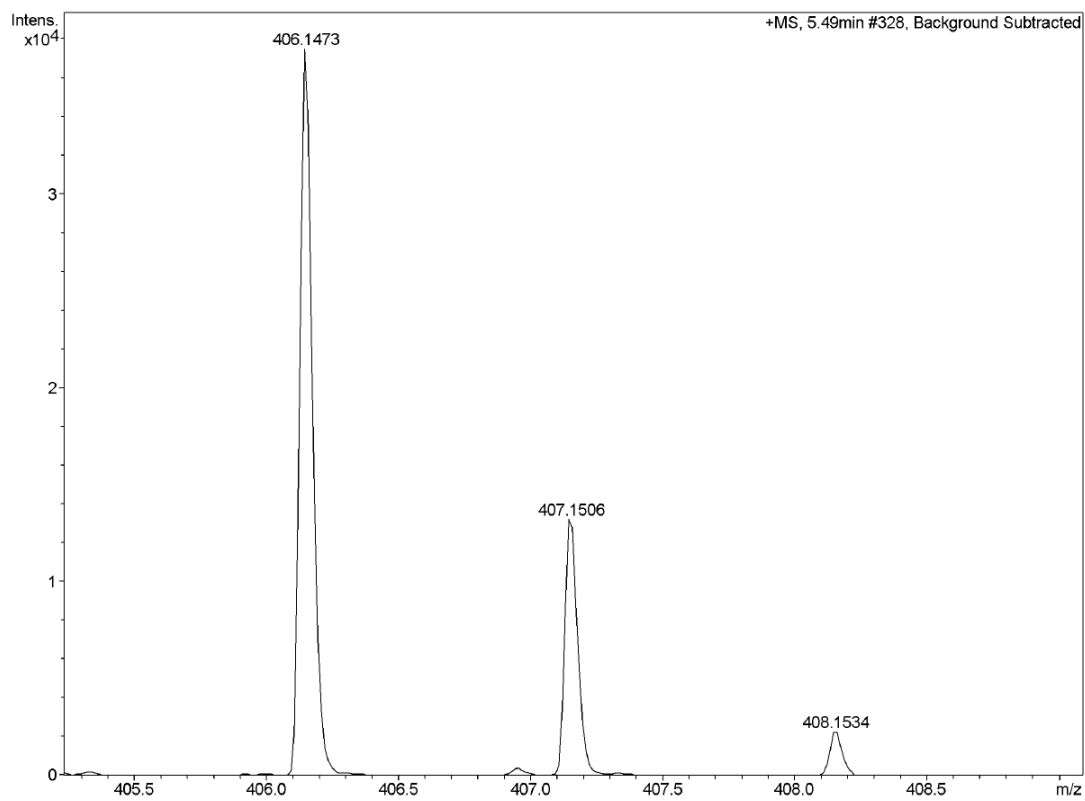


Fig. S43 HR mass spectrum (ESI) of **5b**.

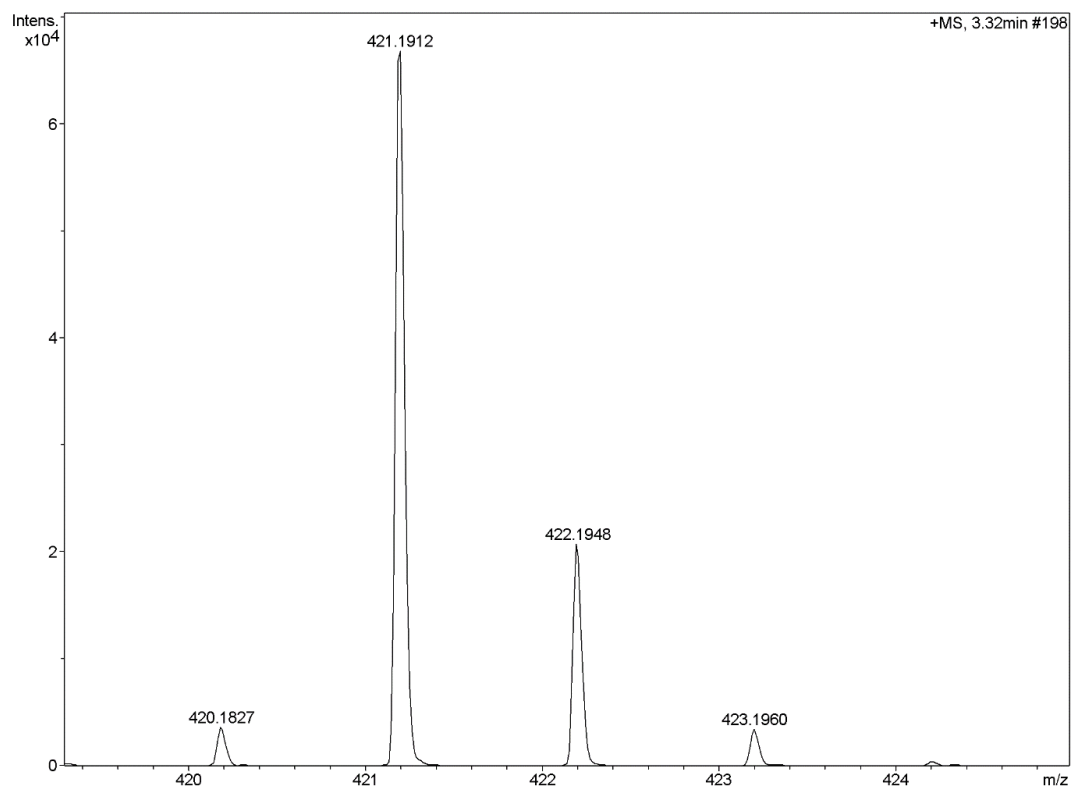


Fig. S44 HR mass spectrum (APCI) of **6a**.

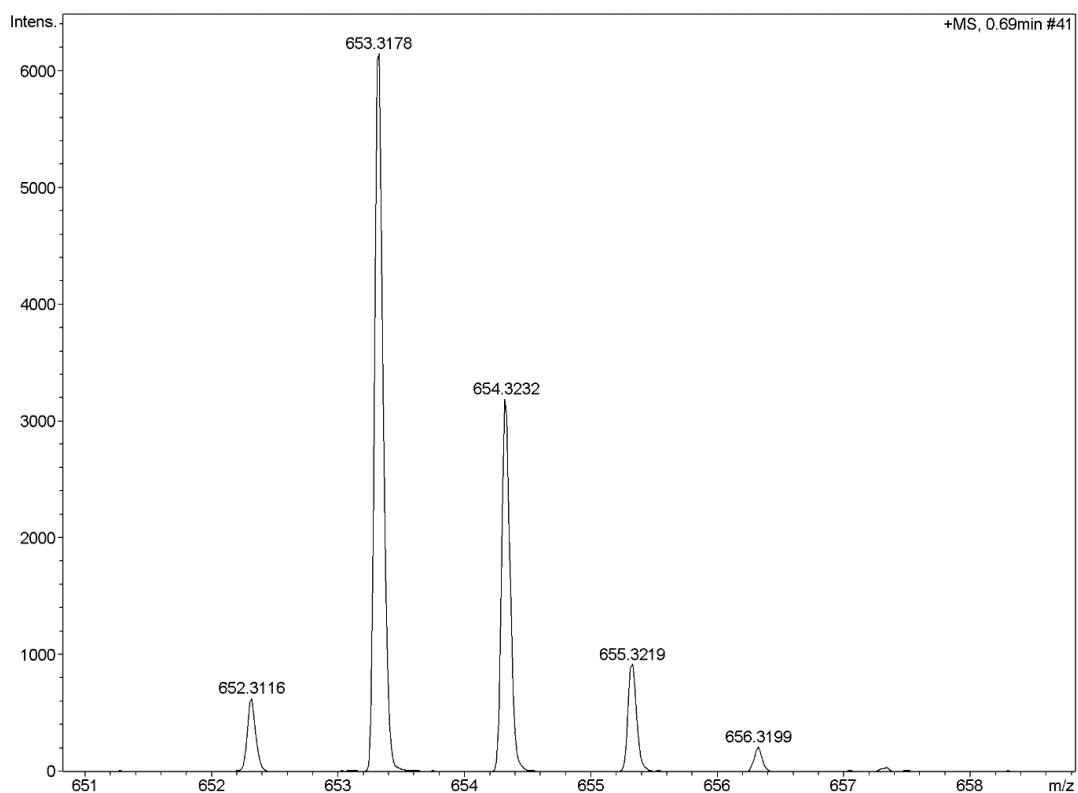


Fig. S45 HR mass spectrum (APCI) of **7a**.

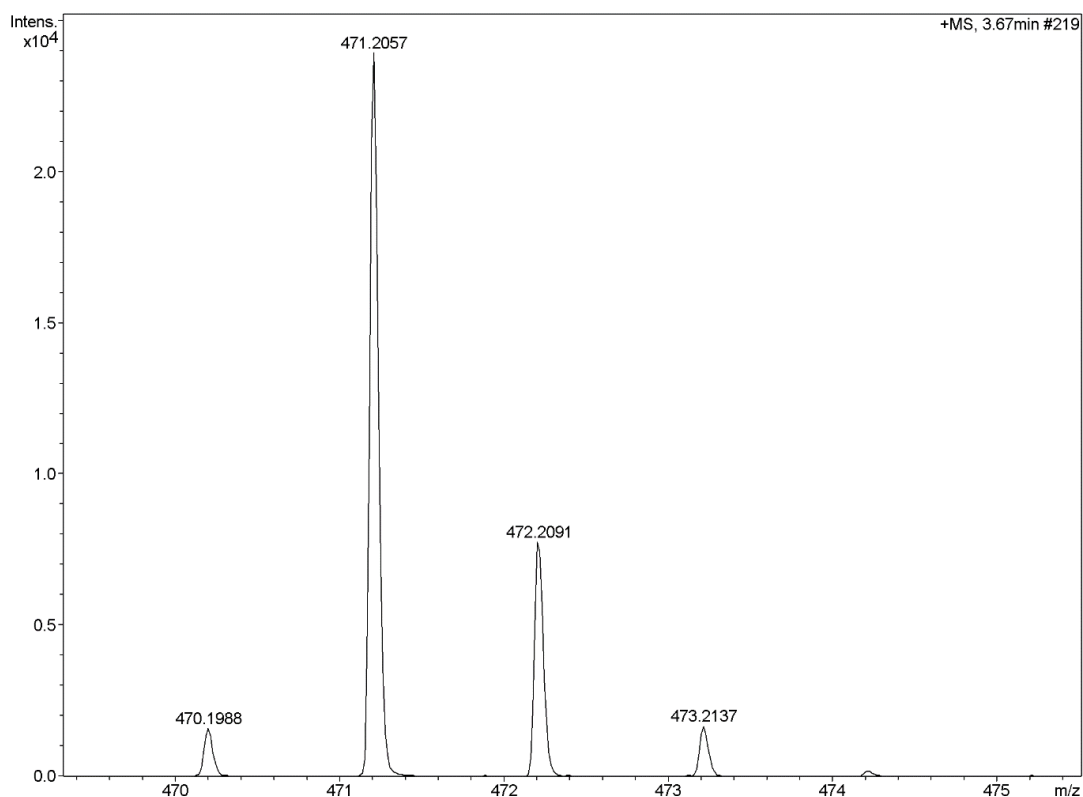


Fig. S46 HR mass spectrum (APCI) of **6b**.

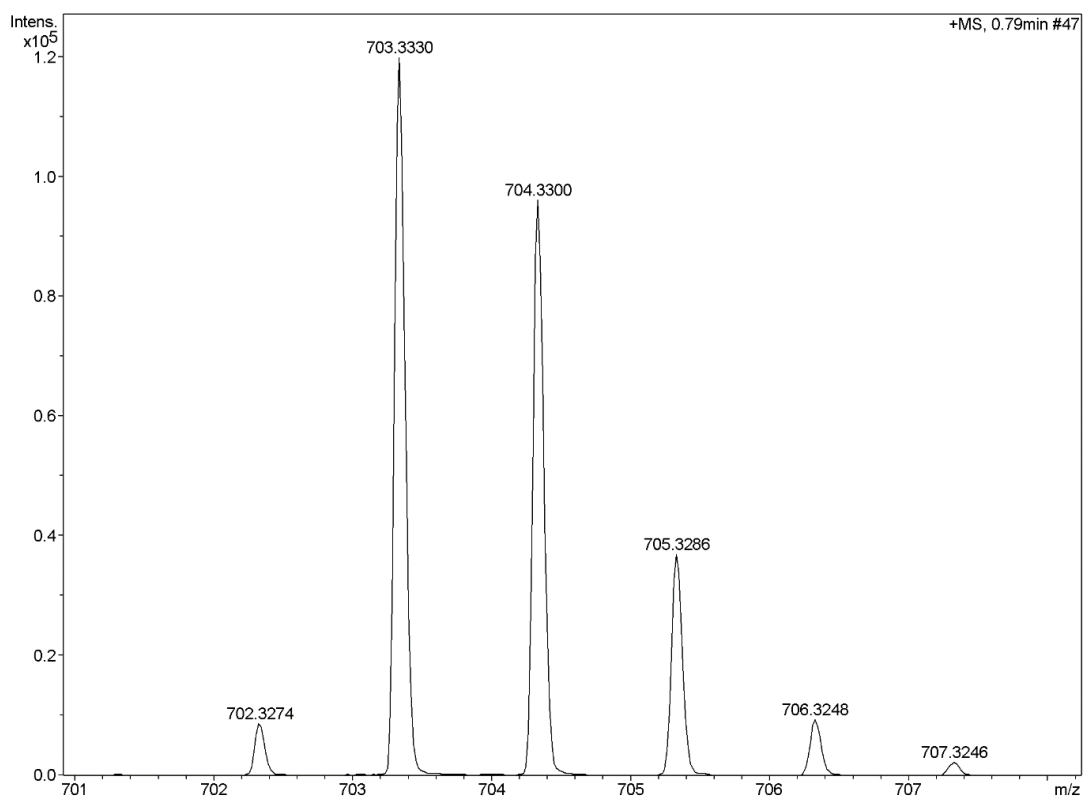


Fig. S47 HR mass spectrum (APCI) of **7b**.

6. References

1. R. Jurok, R. Cibulka, H. Dvořáková, F. Hampl and J. Hodačová, *Eur. J. Org. Chem.*, 2010, **2010**, 5217.
2. Y. B. Borozdina, E. Mostovich, V. Enkelmann, B. Wolf, P. T. Cong, U. Tutsch, M. Lang and M. Baumgarten, *J. Mater. Chem. C*, 2014, **2**, 6618.
3. *Gaussian 09; Revision D.01*; M. J. Frisch, G. W. Trucks, H. B. Schlegel, G. E. Scuseria, M. A. Robb, J. R. Cheeseman, G. Scalmani, V. Barone, B. Mennucci, G. A. Petersson, H. Nakatsuji, M. Caricato, X. Li, H. P. Hratchian, A. F. Izmaylov, J. Bloino, G. Zheng, J. L. Sonnenberg, M. Hada, M. Ehara, K. Toyota, R. Fukuda, J. Hasegawa, M. Ishida, T. Nakajima, Y. Honda, O. Kitao, H. Nakai, T. Vreven, J. A. Montgomery, Jr., J. E. Peralta, F. Ogliaro, M. Bearpark, J. J. Heyd, E. Brothers, K. N. Kudin, V. N. Staroverov, R. Kobayashi, J. Normand, K. Raghavachari, A. Rendell, J. C. Burant, S. S. Iyengar, J. Tomasi, M. Cossi, N. Rega, J. M. Millam, M. Klene, J. E. Knox, J. B. Cross, V. Bakken, C. Adamo, J. Jaramillo, R. Gomperts, R. E. Stratmann, O. Yazyev, A. J. Austin, R. Cammi, C. Pomelli, J. W. Ochterski, R. L. Martin, K. Morokuma, V. G. Zakrzewski, G. A. Voth, P. Salvador, J. J. Dannenberg, S. Dapprich, A. D. Daniels, Ö. Farkas, J. B. Foresman, J. V. Ortiz, J. Cioslowski, and D. J. Fox, Gaussian, Inc., Wallingford CT, **2009**.
4. (a) A. D. Becke, *J. Chem. Phys.* 1993, **98**, 5648. (b) C. Lee, W. Yang, R. G. Parr, *Phys. Rev. B: Condens. Matter* 1988, **37**, 785. (c) T. Yanai, D. Tew and N. Handy, *Chem. Phys. Lett.* 2004, **393**, 51. (d) R. Ditchfield, W. J. Hehre and J. A. Pople, *J. Chem. Phys.* 1971, **54**, 724. (e) W. J. Hehre, R. Ditchfield and J. A. Pople, *J. Chem. Phys.* 1972, **56**, 2257. (f) P. C. Hariharan and J. A. Pople, *Theor. Chim. Acta* 1973, **28**, 213.
5. (a) S. Yamanaka, M. Okumura, M. Nakano and K. Yamaguchi, *J. Mol. Struct.* 1994, **310**, 205. (b) K. Kamada, K. Ohta, A. Shimizu, T. Kubo, R. Kishi, H. Takahashi, E. Botek, B. Champagne and M. Nakano, *J. Phys. Chem. Lett.* 2010, **1**, 937.